Fundamental Concepts of Recharge in the Desert Southwest: A Regional Modeling Perspective

Article · January 2004

DOI: 10.1029/009WSA10

CITATIONS
49

READS
222

4 authors, including:

Alan L. Flint
United States Geological Survey
191 PUBLICATIONS **5,568** CITATIONS
SEE PROFILE

Lorraine E Flint
United States Geological Survey
128 PUBLICATIONS **3,867** CITATIONS
SEE PROFILE

J.A. Hevesi
United States Geological Survey
27 PUBLICATIONS **875** CITATIONS
SEE PROFILE

Fundamental Concepts of Recharge in the Desert Southwest: A Regional Modeling Perspective

Alan L. Flint, Lorraine E. Flint, Joseph A. Hevesi,
U.S. Geological Survey, Sacramento, CA

and Joan B. Blainey
U.S. Geological Survey, Tucson, AZ

Recharge in arid basins does not occur in all years or at all locations within a basin. In the desert Southwest potential evapotranspiration exceeds precipitation on an average annual basis and, in many basins, on an average monthly basis. Ground-water traveltime from the surface to the water table and recharge to the water table vary temporally and spatially owing to variations in precipitation, air temperature, root zone and soil properties and thickness, faults and fractures, and hydrologic properties of geologic strata in the unsaturated zone. To highlight the fundamental concepts controlling recharge in the Southwest, and address the temporal and spatial variability of recharge, a basin characterization model was developed using a straightforward water balance approach to estimate potential recharge and runoff and allow for determination of the location of recharge within a basin. It provides a means for interbasin comparison of the mechanisms and processes that result in recharge and calculates the potential for recharge under current, wetter, and drier climates. Model estimates of recharge compare favorably with other methods estimating recharge in the Great Basin. Results indicate that net infiltration occurs in less than 5 percent of the area of a typical southwestern basin. Decadal-scale climatic cycles have substantially different influences over the extent of the Great Basin, with the southern portion receiving 220 percent higher recharge than the mean recharge during El Niño years in a positive phase of the Pacific Decadal Oscillation, whereas the northern portion receives only 48 percent higher recharge. In addition, climatic influences result in ground-water traveltimes that are expected to vary on time scales of days to centuries, making decadal-scale climate cycles significant for understanding recharge in arid lands.

1. INTRODUCTION

The purpose of this study was to develop a simple model for basin characterization that allows interbasin comparison of recharge mechanisms and the potential for recharge under current, wetter, and drier climates, and to highlight the fundamental concepts and mechanisms that control recharge in the deserts of the Southwestern United States (Southwest). The method developed allows analysis of climate change, as changes in precipitation and air temperature, to evaluate the potential for changes in ground-water recharge in the Great Basin and eventually in other areas in the Southwest. Without further refinements, this modeling approach primarily is intended to provide a means for hydrologically characterizing basins on a basin-wide or regional scale on the basis of fundamental concepts of recharge as they apply to southwestern desert environments. Estimates of recharge in basins of the Great Basin are presented for the purpose of illustrating the approach, evaluating relative proportions of recharge and runoff to describe the dominant mechanisms controlling recharge, and providing a comparison with other methods that have estimated recharge in the Great Basin. They are not relied on as accurate enough at this time to be used for assessment of water availability.

A basin characterization model (BCM) was developed for this study to determine the spatial and temporal variability of net infiltration (all terms are defined below), which is assumed to be equal to recharge because the model assumes steady state con-

Flint, A.L., Flint, L.E., Hevesi, J.A., and Blainey, J.M., 2004, Fundamental concepts of recharge in the Desert Southwest: a regional modeling perspective, in *Groundwater Recharge in a Desert Environment: The Southwestern United States*, edited by J.F. Hogan, F.M. Phillips, and B.R. Scanlon, Water Science and Applications Series, vol. 9, American Geophysical Union, Washington, D.C., 159-184.

ditions and no lateral subsurface flow. The BCM uses a mathematical deterministic water-balance approach that includes the distribution of precipitation and the estimation of potential evapotranspiration, along with soil water storage and bedrock permeability. The BCM was used with available GIS data (digital elevation model, geology, soils, vegetation, precipitation, and air temperature maps), and GIS data that was developed for this study.

The BCM can be used to identify locations and climatic conditions that allow for excess water, quantifying the amount of water available either as runoff or as in-place recharge on a monthly basis, and allows inter-basin comparison of recharge mechanisms. The model does not distinguish between mountain front and stream channel recharge, which are referred to in this paper as runoff, nor does it explicitly define the percentage of runoff that becomes recharge. Because the accurate estimates of recharge cannot be calculated without further refinement to the BCM to estimate the partitioning of runoff, it calculates *potential* in-place recharge and *potential* runoff, and provides the distribution of both in a basin. These values can be combined using assumptions of the amount of runoff that results in recharge to estimate total potential recharge.

A simple calculation of traveltime through the unsaturated zone can be estimated if steady-state conditions are assumed and if unsaturated zone thickness and permeability data are available [*Flint et al.,* 2000]. The BCM can also be used to evaluate the potential for recharge under current, wetter, and drier climates, and is used to evaluate the role of decadal-scale climate cycles (El Niño/La Niña and the Pacific Decadal Oscillation) on recharge at a pixel scale (generally 30–270 meters) across the Southwest.

1.1 Terms and Concepts

Because many terms related to infiltration and recharge often have different meanings to different researchers, the terms used in this paper are defined and are consistent with those in most current literature. Infiltration is the entry into the soil of water made available at the ground surface [*Freeze and Cherry,* 1979]. Net infiltration is the quantity of water that moves below the zone of surface evapotranspiration processes [*Flint et al.,* 2001]. Under steady-state conditions, net infiltration is equal to recharge unless diverted to an area of flow from a spring and thus lost to evapotranspiration; even under this condition, one could argue that some recharge occurs, even if only to a small local or perched aquifer. Percolation (or drainage) is the process by which water moves downward through the unsaturated zone [*Flint et al.,* 2001]. Recharge is the entry into the saturated zone of water made available at the water-table surface [*Freeze and Cherry,* 1979]. Discharge is the removal of water from the saturated zone across the water-table surface [*Freeze and Cherry,* 1979].

Traveltime in the unsaturated zone is the time it takes for water that has become net infiltration to recharge the water table (hours to millennia); it is controlled by net infiltration, the thickness of the unsaturated zone, and the effective porosity of subsurface flow paths [*Flint et al.,* 2000]. As climate changes, the traveltime of infiltrating water through the unsaturated zone may vary; the spatial distribution of recharge also may vary. Recharge that occurs today is spatially variable owing to the thicknesses of soil and alluvium, the thickness of the unsaturated zone, and to the layering and properties of geologic and sediment strata. Recharge is temporally variable owing to changes in processes controlling net infiltration (primarily climate) for time scales of years to centuries.

Recharge is often discussed as dominant within one of the following basin locations: mountain block, diffuse, mountain front, stream channel, and playa lake. Mountain block recharge occurs directly into the underlying bedrock without runoff and is widely distributed in areas of higher mountainous terrain particularly where there is permeable bedrock. Diffuse recharge is areally distributed in alluvial valleys but away from the stream channels (similar to mountain block recharge). Mountain block recharge and diffuse recharge occur in direct response to the infiltration of rainfall and snowmelt and will be referred to in this paper as in-place recharge. In-place recharge also can occur in response to the local-scale lateral redistribution of rainfall and snowmelt following runoff and subsequent overland flow that does not reach the larger stream channels. Water that does not recharge in place is referred to as runoff in this paper. Runoff may become mountain front recharge, which occurs at boundaries between mountain blocks and deeper alluvial valleys, or beneath ephemeral streams as the streams transition from upland areas with thin soils to alluvial valleys and basins with thick soils. Stream-channel recharge occurs in response to focused or coalescing surface-water flows in ephemeral streams away from mountain fronts, or in perennial streams. Playa lake recharge occurs from runoff that collects and eventually evaporates or recharges under the playa (*Stephens*, 1995).

1.2 Study Area

The climate regime of the Southwest is generally considered arid to semi-arid [*UNESCO,* 1979]. Recently, researchers in the United States Geological

Survey (USGS) have been evaluating climate cycles in the Southwest [*Schmidt and Webb*, 2001]. As part of that evaluation a study was initiated to define the boundaries of the "dry" Southwest and to classify each hydrologic basin by climate [*Flint et al.*, 2003]. The United States is divided and sub-divided by the USGS into successively smaller hydrologic units, which are classified into four levels. Surface water drainage divides primarily define the boundaries of the hydrologic units, with the larger drainage systems often subdivided into smaller sub-drainages or areas. Each hydrologic unit is identified by a unique hydrologic unit code (HUC) with the smallest unit having eight digits [*Seaber et al.*, 1987]. The approach to assessing the climate regime is to evaluate the relation between precipitation and potential evapotranspiration in each of these eight-digit HUCs using an international arid land classification index. The Man and the Biosphere Program under the direction of the United Nations Educational, Scientific, and Cultural Organization [*UNESCO*, 1979] developed a method based on the ratio of annual precipitation to potential evapotranspiration. The UNESCO method produces five classes based on this ratio: hyper-arid (< 0.05), arid (0.05-0.2), semi-arid (0.2-0.5), dry-subhumid (0.5-0.65), and humid (>0.65). In order to define a study area for application of the BCM in an arid or semi-arid environment, these classes were applied to the average conditions for eight-digit HUCs defined by the USGS for the Southwest (Plate 1). There are areas that are calculated to be hyper-arid on a grid cell basis, such as Death Valley, that do not appear when averaged for an entire basin.

The Great Basin represents an arid environment and is centrally located within the Southwest. It was selected for a preliminary analysis to determine the feasibility of applying a simple basin characterization model for estimating recharge because of the ability to compare it to previous analyses of recharge in the Great Basin. The Great Basin study area is 374,218 km^2 and contains a total of 258 hydrologic units (hydrographic areas and subareas), which will be referred to as basins in this paper (Figure 1). Net infiltration or recharge has been estimated by previous investigators for the basins within the Great Basin using methods such as chloride mass balance [*Dettinger*, 1989], transfer equations based on other variables, such as precipitation using the Maxey-Eakin method [*Maxey and Eakin*, 1950; *Harrill and Prudic*, 1998], basin discharge estimates using evapotranspiration [*Nichols*, 2000], and water-balance and soil physics techniques [*Hevesi et al.*, 2002; *Hevesi et al.*, 2003].

1.3 Conceptual Model

A conceptual model of recharge is essential for developing the GIS-based BCM (Figure 2) [*Flint et al.*, 2001]. The conceptual model for a basin can be simplified to identify areas within a basin where recharge processes are initiated. Recharge does not occur everywhere in a basin nor does it occur each year. It is likely that the majority of the area contributing to recharge is a relatively small portion of the basin and years with above average precipitation and snow accumulation provide the most recharge [*Flint et al.*, 2001]. The BCM is used to identify those areas and climate conditions that are conducive to direct recharge or to runoff (which, in turn, could lead to recharge downstream). In discussion of a conceptual model, the term net infiltration is used to describe the surface processes, whereas the BCM assumes steady state conditions and net infiltration is equal to recharge.

For most of the Southwest on a yearly basis, and in most basins on a monthly basis, potential evapotranspiration exceeds precipitation [*Flint et al.*, 2003]. However, in certain areas of a basin (in particular, for the higher elevations), precipitation can exceed potential evapotranspiration and storage and net infiltration and/or runoff may occur, depending on the rate of rainfall or snowmelt, soil properties (including permeability, thickness, field capacity, and porosity), and bedrock permeability. For many basins, snow accumulated for several months provides enough moisture to exceed the soil storage capacity and exceed potential evapotranspiration for the month or months during which snowmelt occurs.

The conceptual model assumes that all processes controlling net infiltration occur within the top 6 m of the surficial materials as shown by *Flint and Flint* [1995] for Yucca Mountain in the southern Great Basin. This is a conservative estimate for the Southwest, and is only likely to occur in riparian zones where deeper-rooted vegetation can retrieve water that has penetrated deeper than six meters. Although these zones are an extremely small percentage of the area in the Southwest, and particularly the Great Basin, if high resolution information on vegetation type for these areas is available, the model should be adjusted to use the appropriate rooting depth. The alternate process of exfiltration in arid environments whereby water is drawn upward from the soil profile under vapor density gradients and evaporates at the surface to provide a negative water balance, although important in characterizing deep alluvium, is considered negligible on a basin or regional scale for the purposes of this analysis.

The BCM uses spatially distributed estimates of monthly precipitation, monthly air temperature, monthly potential evapotranspiration, soil water storage, and bedrock permeability to determine the area

in a basin where excess water is available. Potential evapotranspiration is modeled and partitioned on the basis of vegetation cover to represent bare soil evaporation and vegetation evapotranspiration. Depending on the soil and bedrock permeability, excess water is partitioned as either (1) in-place recharge, or (2) runoff that can potentially become mountain front recharge or stream channel recharge either at the mountain front or farther downstream in the alluvial basin.

Net infiltration occurs when enough water is made available to exceed the storage capacity of the soil (or rock); precipitation, snowmelt, or run-on provide the water; root zone, soil depth, porosity, and the soil drainage characteristics provide the storage; vegetation, bare soil surfaces, and the energy balance control potential evapotranspiration, which decreases soil water content thus increasing soil water storage between precipitation/snowmelt/run-on events. The topography and atmospheric conditions control much of the energy available for potential evapotranspiration.

For thin soils underlain by fractured bedrock the soil water content will approach saturation because the water entry potential of the fracture network must be exceeded before significant drainage into the underlying bedrock can occur (the fracture network is a capillary barrier to drainage from the soil). In locations with thick soil a greater volume of water is needed (compared to thin soil locations) to exceed the storage capacity of the root zone, which is deeper relative to locations with thin soil, (or the permeability must be high enough to quickly drain the root zone (e.g., young gravelly channels)). In general, bedrock permeability, soil storage capacity, and evapotranspiration are the factors that determine the vertical direction of water flow. In upland areas with thin soils, soil thickness is the most important factor affecting soil storage capacity. If the soil is thin and bedrock permeability is low then evapotranspiration has more time to remove stored water between precipitation, snowmelt, and run-on events. If the bedrock permeability is high then evapotranspiration has less time to remove stored water between events. In alluvial fans, basins, and valleys with thick soils and deeper root zones, if the soil field capacity is high and the permeability is low (for example, finer grained soils) then drainage through the root zone occurs slowly and evapotranspiration has more time to remove stored water between events. If the soil field capacity is low and the permeability is high (coarser grained soils) then drainage through the root zone occurs more rapidly and evapotranspiration has less time to remove stored water between events.

Where net infiltration occurs in the Southwest is very important, particularly if one intends to quantify or analyze it by means of field measurements. For example, measuring stream flow losses or calculating Darcy flux from data obtained under a stream channel would not provide an accurate estimate of recharge in a basin dominated by in-place recharge processes. To determine approximately where recharge is occurring and what mechanisms dominate, all available information was assembled (GIS coverages), combined with the conceptual model, to calculate locations within a basin where recharge is likely to occur. Because the spatial and temporal distribution of net infiltration is dependent on precipitation, soil water storage, bedrock permeability, and evapotranspiration, all of which can be estimated with available data on a regional scale, the most probable locations for potential in-place recharge and potential runoff can be identified. In the BCM, potential in-place recharge is calculated as the maximum volume of water for a given time frame that can recharge directly into bedrock or alluvium. Potential runoff is the maximum volume of water for a given time frame that will run off the mountain front or become streamflow. Total potential recharge is the combination of in-place recharge and runoff and assumes that all runoff becomes recharge. Analyses of basins using the water balance approach in the BCM can help determine when, where, and how the water-balance terms, the material properties, and the physical mechanisms can be combined to produce net infiltration or recharge.

1.4 Recharge and Groundwater Traveltime

An important issue to be addressed is the timing of recharge after net infiltration occurs. It is quite likely that if predictions of drier climate over the next 20 years [*Schmidt and Webb,* 2001] prove to be true, that this would reduce net infiltration values both spatially and temporally. It is also likely that some basins will not experience a change in recharge related to this climate change for hundreds or thousands of years. Therefore, an analysis of unsaturated zone traveltime is needed to determine when changes in surface processes will be reflected at the water table. Assuming negligible traveltime for net infiltration from 0-6 m and vertical flow through the unsaturated zone, traveltime is controlled by the net infiltration rate, unsaturated zone thickness, the effective porosity of the flow path, and the lowest permeability encountered along a given flow path (which would determine the maximum net infiltration rate at which the assumption of vertical flow would still apply). Unsaturated zone traveltime controls the timing of recharge; therefore ground-water responses to changes in climate (seasonal, yearly, or decadal) may

be delayed, suggesting important implications for water availability under future climate scenarios.

Unsaturated zone traveltime can be calculated as $(\phi_{eff} Z_{uz})/ I_{net}$, where ϕ_{eff} is effective unsaturated zone porosity (m/m), Z_{uz} is the thickness of the unsaturated zone (m), and I_{net} is net infiltration (m/yr) [*Flint et al.*, 2000]. *Flint et al.* [2000] estimated the thickness of the unsaturated zone in the Death Valley region on the basis of the difference in elevation determined using a digital elevation model and the spatially interpolated water-table elevation. The effective unsaturated zone porosity is the most difficult parameter to assess. It can be evaluated using detailed geologic maps from the surface to the water table and an estimate of the porosity of the rock matrix and(or) fractures of the geologic material. An estimate of subsurface bedrock permeability of the matrix can also be useful in helping to estimate effective unsaturated zone porosity. If the estimated net infiltration is less than the matrix permeability then the flow is likely in the matrix and matrix saturation becomes a good estimate for ϕ_{eff}. If net infiltration is more than matrix permeability then the flow is likely in the fractures. In this case, an estimate of fracture porosity becomes a good estimate for ϕ_{eff}. Either case can help determine whether a high porosity (matrix flow dominated) or a much lower porosity (fracture flow dominated) should be used.

Flint et al. [2000] showed traveltime delays of 10's to 1,000's of years for the southern Great Basin due to variation in net infiltration rates and the thickness of the unsaturated zone, which is commonly 10-100 m thick, but can exceed 2,000 m in thickness. Although parts of the regional flow system may respond quickly to climate change, others may lag behind significantly. This variability may be significant in determining the rate and direction of groundwater flow and the resultant availability of groundwater as a resource.

2. METHODS

2.1 Water-balance Calculations

A series of water-balance equations were developed to calculate the area and the amount of potential recharge. For example, each model grid cell was analyzed for each month to determine water availability for recharge. This available water (AW) for potential recharge, potential runoff, or water to be carried over to the following month is defined as

$$AW = P + S_m - PET - S_a + S_s \quad (1)$$

where P is precipitation, S_m is snowmelt, PET is potential evapotranspiration, S_a is snow accumulation and snow pack carried over from the previous month, and S_s is stored soil water carried over from the previous month. All units are in millimeters per month. Potential runoff was calculated as the available water minus the total storage capacity of the soil (soil porosity multiplied by soil depth). Potential in-place recharge was calculated as the available water remaining (after runoff) minus the field capacity of the soil (the water content at which drainage becomes negligible). Maximum in-place recharge on a unit grid cell basis is the permeability of the bedrock (cm^3 of water per cm^2 grid cell area per month). If the total soil water storage is reached, the potential in-place recharge is equal to the bedrock permeability. Any water remaining after the monthly time step would be carried over into the next month in the S_s term.

Soil water storage capacity and soil infiltration capacity were estimated using soil texture estimates from the State Soil Geographic Database (STATSGO; http:// www.ftw.nrcs.usda.gov/stat_data.html), a state-compiled geospatial database of soil properties that generally are consistent across state boundaries [*U. S. Dept. of Agriculture-National Resource Conservation Service*, 1994]. Soil thickness was estimated using available geologic maps to estimate soil depths of 6 m wherever quaternary alluvial deposits were mapped [*Hevesi et al.*, 2003]. Everywhere else, the STATSGO database was used, which provides soil depths to 2 m. Bedrock permeability was estimated using a bedrock geologic map and literature values for the estimation of permeability on the basis of geologic material [*Bedinger et al.*, 1989]. Macropore and fracture flow is considered within the bedrock permeability estimation, which assumes values on the basis of measured bulk permeabilities at the surface or borehole transmissivities. Uncertainties in soil and bedrock properties are discussed in *Hevesi et al.*, [2003].

The ratio of potential runoff versus potential in-place recharge determines whether mountain front and(or) stream channel recharge mechanisms dominate relative to in-place recharge in response to rainfall and snowmelt (in other words, the significance of surface-water flow to total recharge increases as the ratio of runoff to mountain block recharge increases). This ratio does not determine where the runoff infiltrates so it can not distinguish between mountain front or stream channel recharge that may occur farther into the basin. The BCM model allows snow pack and soil moisture to be carried over from month to month, which becomes important when temperatures are cold enough for precipitation to form snow. Since snow may persist for several months before melting, large volumes of water may be made avail-

able for potential recharge in a single monthly model time step.

2.2 Climate Distribution

Climate was simulated in this study for the Great Basin using two approaches to evaluate the difference in recharge estimates between (1) average climate conditions for 34 years, January 1, 1956, through December 31, 1999, where spatially distributed estimates of mean monthly precipitation and mean monthly maximum and minimum air temperature were used, and (2) time-varying climate conditions, where spatially distributed estimates of monthly precipitation and maximum and minimum monthly air temperatures for the 34 year period were used. These estimates were made using historical daily precipitation and air temperature data from a network of 448 monitoring stations in and adjacent to the Great Basin [*National Climatic Data Center*, 2000a,b] that existed between 1900-1999. Approximately 300 stations were active at any given time for the 34 year period. The measured values of precipitation and minimum and maximum air temperature were spatially distributed to all the grid cells for the Great Basin model domain (270 x 270 m) using a model from *Nalder and Wein* [1998] that combines a spatial gradient plus inverse distance squared weighting to monthly point data to interpolate to each grid cell with multiple regression. Parameter weighting is based on location and elevation following the equation:

$$Z = \left[\sum_{i=1}^{N} \frac{Z_i + (X - X_i) \times C_x + (Y - Y_i) \times C_y + (E - E_i) \times C_e}{d_i^2} \right] / \left[\sum_{i=1}^{N} \frac{1}{d_i^2} \right]$$

where Z = estimated climatic variable, Zi is the value of climate station I, Xi, Yi, Ei are easting, northing, elevation of climate station I, N is the number of climate stations, Di is the distance from the site to climate station I, and Cx, Cy, Ce are regression coefficients for easting, northing, elevation.

Snow depth was calculated for areas where precipitation occurs and air temperature is at or below freezing. Sublimation of snow was calculated as a percentage of evapotranspiration, and snowmelt was based on net radiation when air temperatures were above freezing.

2.3 Potential Evapotranspiration

Potential evapotranspiration was estimated using a computer program modified from *Flint and Childs* [1987] that calculates solar radiation for each grid cell in the model domain, and when combined with air temperature, is converted to net radiation and soil heat flux [*Shuttleworth*, 1993]. The result was used with the Priestley–Taylor equation [*Priestley and Taylor*, 1972] to estimate potential evapotranspiration, and was corrected for vegetated and bare soil area using estimates of vegetation cover from vegetation maps (National Gap Analysis Program; http://www.gap.uidaho.edu). Actual evapotranspiration is a function of soil moisture and is more rigorously addressed in *Hevesi et al.* [2002, 2003]. The regional scale approach used with the BCM assumes that potential evapotranspiration can be used to provide a potential estimate of recharge to bound the values for evaluating mechanisms and differences among basins. Following refinement and the incorporation of actual evapotranspiration in the BCM, recharge can more accurately be estimated for more intensive applications.

2.4 Basin Application

The BCM code is written in FORTRAN-90, and uses ASCII files of distributed upper boundary conditions and GIS grid files of surface properties as input for the calculations of potential recharge and potential runoff. The BCM was applied to the Great Basin using the two different simulation scenarios (mean monthly climate and 34-year monthly time series from 1956-1999) to evaluate the relative amount of recharge and the mechanisms that would dominate under wetter or drier climatic conditions. Consideration of snow accumulation can be critical because the accumulation can delay the application of water to the surface thus extending the possibility that in the following month the combination of precipitation and snowmelt will exceed the storage capacity of the soil causing net infiltration and(or) runoff. The BCM estimates for the Great Basin were compared with recharge estimates determined using the Maxey–Eakin approach from *Harrill and Prudic* [1998], chloride-mass balance estimates of *Dettinger* [1989] published in *Harrill and Prudic* [1998] for the Great Basin, basin discharge estimates determined using evapotranspiration [*Nichols*, 2000], and net infiltration estimates determined using a daily water-balance model *Hevesi et al.* [2002, 2003].

3. RESULTS AND DISCUSSION

Total mean annual potential recharge (mean annual potential recharge plus potential runoff) estimates were made on a grid cell basis for 258 basins in the Great Basin and are presented in Plate 2. Total mean annual potential recharge for each basin is presented in Plate 3 and Table 1. The results shown in Figure 4 indicate that most of the in-place recharge or runoff occurs at, or is generated from, the basin boundaries.

This was an expected result because the basin boundaries primarily occur along the drainage divides, and the divides tend to have higher elevations (thus higher precipitation and lower air temperature) and thinner soils relative to the soils in the central part of each basin.

3.1 Evaluation of Recharge Processes

Results of the mean monthly calculations indicate that there is 2.41 million acre-feet/year of potential in-place recharge in the Great Basin and 4.83 million acre-feet/year of potential runoff, or a total potential recharge of 7.24 million acre-feet/year. Results of the 34-year time series calculations indicate that there is slightly more recharge when water can be carried over between months: 2.43 million acre-feet/year of potential in-place recharge, and 5.24 million acre-feet/year of potential runoff, or a total potential recharge of 7.67 million acre-feet/year. Although the amount of recharge that occurs as a result of runoff is not known, based on analyses performed by *David Prudic* [*U.S. Geological Survey, personal communication,* 2001] and *Hevesi et al*. [2003], it was assumed that about 10 percent of runoff becomes recharge in the southern part of the Great Basin and as much as 90 percent in the northern part. This results in a total potential recharge for the 34-year time series of 2.95 million acre-feet/year. This is a conservative estimate, as it currently is not known what the spatial or temporal distribution of the recharge portion of runoff is. The percentage is probably a function of the timing of precipitation and snowmelt, topographic position, and the hydrologic properties of alluvium and bedrock, and deserves further investigation during future BCM refinement.

Grid-based estimates of the ratio of potential in-place recharge to potential runoff are presented in Plate 4, the ratio of the calculated means of potential in-place recharge to potential runoff for each basin is presented in Plate 5. The ratio of potential in-place recharge to potential runoff provides an indication of the mechanisms that likely are dominant in controlling recharge. The grid-based analysis provides the distribution within basins of the dominant mechanisms, whereas the mean basin values provide a larger scale representation for basin comparison and regional analysis. A ratio of 0.5 or less indicates that more than twice as much water has the potential to become runoff than to become in-place recharge. A ratio of 2.0 or greater indicates that water has at least twice as much potential to become in-place recharge than to become runoff. An example of the control that bedrock type, and thus bedrock permeability, has on the calculation of recharge is apparent in Plate 5 with the observation that the major assemblage of basins in which in-place recharge is dominant (> 2.0) (noted as extending from the southern portion of the Great Basin through the central region and to the northeast), coincides with the carbonate-rock province which is dominated by high permeability bedrock. The role that bedrock plays in the determination of recharge mechanisms is supported with the use of a detailed water-balance model for the Death Valley region by *Hevesi et al*. [2002], which showed much higher recharge in basins dominated by carbonate rock and lower recharge in basins dominated by thick soils and lower permeability volcanic rock types [*Hevesi et al.*, 2002; Figure 9].

3.2 Effect of Climate Variability

The role of climate variability is highlighted in an evaluation of potential recharge in two basins, Continental Lake Valley in the northern Great Basin, and Valjean Valley in the southern Great Basin (Plate 5). The total potential recharge is about 2,000 acre-feet/year for Continental Lake Valley and about 270 acre-feet/year for the Valjean Valley (Table 1). These values were calculated as all the in-place recharge plus 10 percent of runoff, using the 34-year time series approach. To illustrate the climatic conditions responsible for the resultant difference in recharge between the basins, the percentage deviation in annual potential recharge from the mean is shown in Figure 3, calculated as the difference between the total potential recharge for each year and the mean total potential recharge for the 34-year period from 1956-1999. The 34-year simulation period includes positive and negative phases of the Pacific Decadal Oscillation (PDO), a southern oscillation index of an approximately 40-year climatic cycle, and several El Niño cycles [*Dettinger et al.*, 2000]. Both basins appear to be influenced by the shift in the PDO in 1977 from a negative phase to a positive phase, and both basins are influenced by El Niño years, noted as open diamonds, during the positive PDO, although the influence is much stronger in the Valjean Valley. During El Niño years with a positive PDO, the mean annual total potential recharge in the Valjean Valley is about 220 percent higher than the 34-year mean; during El Niño years with a negative PDO, recharge is about 13 percent lower (recharge for all the years with a positive PDO is about 55 percent higher than the 34-year mean, and recharge for all the years with a negative PDO is about 48 percent lower) (Figure 3). In the Continental Lake Valley, annual total potential recharge for the El Niño years with a positive PDO is about 48 percent higher than the 34-year mean, and recharge for El Niño years with a negative PDO is about 43 percent lower (recharge during all years with a positive PDO is about 37 percent higher

than the 34-year mean, and recharge during all the years with a negative PDO is about 37 percent lower). A comparison of annual total potential recharge estimated for non-El Nino years with the mean recharge for 1956 through 1999 showed that non-El Nino recharge was 97 percent lower than the 34-year mean for the Valjean Valley and 46 percent lower for the Continental Lake Valley. This suggests that actual climate data rather than a mean value for recharge should be used in the BCM.

The influence of climate on recharge can also be seen on a plot comparing the percentage deviation of mean annual total potential recharge from the 34-year mean and the percentage deviation of mean annual precipitation from the 34-year mean for the Valjean Valley and the Continental Lake Valley basins. The range of precipitation for the Valjean Valley is much wider than that for the Continental Lake Valley because of the stronger influence of El Niño years in the southern part of the Great Basin (Figure 4). This results in more scatter in the recharge estimates for years with high precipitation and occasionally much more recharge.

The expected climate conditions for the next 20 years, which have not yet been modeled, probably will provide less snow accumulation in the higher elevations [*Schmidt and Webb,* 2001] and therefore less net infiltration, which would greatly reduce the potential for mountain block and mountain front recharge. If the predicted warmer and drier climate occurs, recharge during the next 20 years will result in lower net infiltration to desert-basin aquifers, which eventually would result in lower recharge; the response to the predicted climate may be delayed 10s to 1000s of years. Only where traveltimes in the unsaturated zone are less than 20 years would there be a response to recharge for the drier and warmer climate scenario. When the details of the climate scenarios are better defined, the BCM can be used as a more direct indicator of recharge for each basin.

3.3 Comparison with Other Methods

Total potential recharge (shown on a log scale) calculated for 258 basins in Table 1 is presented in Plate 6, sorted from lowest to highest recharge calculated using the BCM and the 34-year time series approach. Estimates of total potential recharge, calculated as mean in-place potential recharge plus 10 percent of the potential runoff using the BCM was compared with estimates of recharge made using the Maxey–Eakin method [*Harrill and Prudic,* 1998], the chloride-mass balance method [*Dettinger,* 1989], and the daily water-balance model of *Hevesi et al.* [2002 (INFILv1); 2003 (INFILv3)]. The BCM improves estimates over that of the Maxey–Eakin method because it takes into account the spatially distributed features of the surface, such as bedrock permeability and soil storage capacity, as well as potential evapotranspiration, rather than only precipitation. The remaining methods compare to the BCM time-series results within an order of magnitude, with the exception of one chloride mass balance point and one water-balance model (INFILv1) point. The BCM results using the average monthly conditions have less total potential recharge for about half of the basins.

The range of estimates for each basin is indicated by a bar that is constructed by subtracting the 10 percent of runoff that is assumed to become recharge (which then assumes that no runoff results in recharge), and adding the other 90 percent (which then assumes that all runoff results in recharge). This results in a range of estimates for each basin that reflects the possible assumptions of no runoff resulting in recharge to all runoff resulting in recharge. The large range in total potential recharge given the possible assumptions regarding runoff, particularly at the higher recharge rates, indicates the need to further develop the BCM to differentiate between and quantify runoff that occurs in the mountain front areas to become recharge and the amount of runoff in the streams that becomes recharge. The red diamonds in Plate 6 show the results of the BCM determined using mean monthly climate estimates for a 12-month period rather than the monthly time series for a 34-year period. The basins with the largest recharge values have very similar estimates using either the time series or the monthly averages.

4. SUMMARY

Recharge is temporally and spatially variable and is controlled, to a large extent, by the near surface process of net infiltration. Net infiltration is a function of precipitation, air temperature, root zone and soil properties and depth, and bedrock permeability. Present-day net infiltration is assumed to be equivalent to potential future recharge on a regional basis but can be significantly delayed by traveltime through the unsaturated zone. The monthly water-balance method presented here provides a straightforward approach to compare the potential for net infiltration between basins for current or different climates. If using mean monthly precipitation, potential recharge in the Great Basin is estimated to be between 2.41 million acre-feet/year (including only in-place potential recharge) and 7.24 million acre-feet/year (including in-place potential recharge plus all potential runoff). Total estimated potential recharge including only 10 percent of potential runoff is 2.89 million acre-feet/year. A mean annual precipi-

tation produces less recharge than the mean of the time series of years making climate variability an important consideration in analyzing recharge in desert environments. These calculations result in potential recharge estimated to be between 2.43 million acre-feet/year (including only in-place potential recharge) and 7.67 million acre-feet/year (including in-place potential recharge plus all potential runoff). Total estimated potential recharge including only 10 percent of potential runoff is 2.95 million acre-feet/year. Because net infiltration and recharge are temporally and spatially variable and often only occurs in 5 percent of a basin, an a priori estimate of the mechanisms and processes contributing to recharge and locations it occurs are an important precursor to locating field measurements used to quantify actual recharges rates.

Additional research is necessary to refine the BCM for use in providing more accurate estimates of in-place recharge and runoff, and particularly to quantify and differentiate between runoff that occurs in shallow alluvium at the mountain front or in ephemeral streams, and runoff that occurs in deeper alluvium under ephemeral or perennial stream channels. In addition, the apparent importance of using a time-series analysis in characterizing desert recharge suggests that a daily time scale would result in even more realistic estimates of recharge and runoff, better capturing the time scale at which precipitation and snowmelt occurs. Surface routing of water to adjacent grid cells would also improve the estimates of surface infiltration, especially if the BCM were used on a fine grid scale, such as 10 or 30 m. These refinements would likely require the use of coding for parallel processing for application of the BCM to basin-scale or regional-scale analyses. Finally, although it is beyond the scope of this paper to address this topic fully, the changes in vegetation type, density, and rooting depth, particularly in riparian zones, that likely would occur with decadal-scale changes in climate should be taken into consideration alongside the development of climate scenarios to include the associated changes in potential evapotranspiration.

REFERENCES

Bedinger, M.S., Langer, W.H., and Reed, J.E., 1989, Ground-water hydrology: *in* Bedinger, M.S., Sargent, K.A., and Langer, W.H., eds., Studies of geology and hydrology in the Basin and Range Province, Southwestern United States, for isolation of high-level radioactive waste--Characterization of the Death Valley region, Nevada and California, U.S. Geological Survey Professional Paper 1370-F, 49 p.

Dettinger, M.D., 1989, Reconnaissance estimates of natural recharge to desert basins in Nevada, U.S.A., by using chloride-balance calculations: Journal of Hydrology 106:55-78.

Dettinger, M.D., Cayan, D.R., McCabe, G.J., and Marengo, J.A., 2000, Multiscale streamflow variability associated with El Nino/Southern Oscillation: *in* Diaz, H.F. and Markgraf, V. (eds.), El Nino and the Southern Oscillation; multiscale variability and global and regional impacts, Cambridge Univ. Press, Cambridge, U.K., p. 113-147.

Flint, A.L., Blainey, J.B., Flint, L.E., and Haltom, T.A., 2003, Hydrologic analysis of basins in the desert Southwest: U.S. Geological Survey Water-Resources Investigation Report, in review.

Flint, A.L., Flint, L.E., Hevesi, J.A., D'Agnese, F., and Faunt, C., 2000, Estimation of regional recharge and traveltime through the unsaturated zone in arid climates: *in* Faybishenko, B., Witherspoon, P., and Benson, S., (eds.), Dynamics of fluids in fractured rock, Geophysical Monograph 122, American Geophysical Union, Washington, DC, p 115-128.

Flint, A.L., Flint, L.E., Hevesi, J.A., and Hudson, D.B., 2001, Characterization of Arid Land Infiltration Processes at Yucca Mountain, Nevada: *in* D.D. Evans, T.C. Rasmussen, and T.J. Nicholson, (eds.), Flow and Transport through Unsaturated Fractured Rock, Geophysical Monograph 42, American Geophysical Union, Washington, DC, p.135-149.

Flint, A.L., and Childs, S.W., 1987, Calculation of solar radiation in mountainous terrain: Journal of Agricultural and Forest Meteorology, 40:233-249.

Flint, L.E. and Flint, A.L., 1995, Shallow infiltration processes at Yucca Mountain-- Neutron logging data 1984-93: U.S. Geological Survey Water-Resources Investigations Report 95-4035, 46 p.

Freeze, R.A., and Cherry, J.A., 1979, Groundwater: Prentice-Hall, Inc., Englewood Cliffs, N.J., 604 p.

Harrill, J.R., and Prudic, D.E., 1998, Aquifer systems in the Great Basin Region of Nevada, Utah, and Adjacent States—Summary Report: U.S. Geological Survey Professional Paper 1409-A, 66 p.

Hevesi, J.A., Flint, A.L., and Flint, L.E., 2002, Preliminary estimates of spatially distributed net infiltration and recharge for the Death Valley region, Nevada-California: USGS Water Resources Investigation Report 02-4010, 36 p.

Hevesi, J.A., Flint, A.L., and Flint, L.E., 2003, Simulation of net infiltration using a distributed parameter watershed model for the Death Valley regional flow system, Nevada and California: USGS Water Resources Investigation Report 03-4090, 104 p.

Maxey, G.B., and Eakin, T.E., 1950, Ground water in White River Valley, White Pine, Nye, and Lincoln Counties, Nevada: Nevada State Engineer, Water Resources Bulletin 8, 59 p.

Nalder, I.A., and Wein, R.W., 1998, Spatial interpolation of climatic Normals: test of a new method in the Canadian boreal forest: Agric. and Forest Meteor. 92(4): 211-225.

National Climatic Data Center, 2000a, Summary of the Day Observations. 3200-series data. Asheville, North Carolina: NOAA (National Oceanic and Atmospheric Administration). Compiled for proprietary distribution

on 2 Compact Disks "West 1: California, Nevada, Utah, Arizona, New Mexico, Colorado and Wyoming." Boulder, Colorado: EarthInfo, Inc.

National Climatic Data Center, 2000b, Summary of the Day Observations. 3200-series data. Asheville, North Carolina: NOAA (National Oceanic and Atmospheric Administration). Compiled for proprietary distribution on 4 Compact Disks "West 2: for Alaska, Hawaii, Idaho, Kansas, Montana, North Dakota, Nebraska, Oklahoma, Oregon, Pacific Islands, South Dakota, Texas, Washington." Boulder, Colorado: EarthInfo, Inc.

Nichols, W.D., 1987, Geohydrology of the unsaturated zone at the burial site for low level radioactive waste near Beatty, Nye County, Nevada: U.S. Geological Survey Water-Supply Paper 2312, 52 p.

Nichols, W.D., 2000, Regional Ground-Water Evapotranspiration and Ground-Water Budgets, Great Basin, Nevada: U.S. Geological Survey Professional Paper 1628, 82 p.

Priestley, C.H.B., and Taylor, R.J., 1972, On the assessment of surface heat flux and evaporation using large-scale parameters: Manual Weather Review, 100: 81–92.

Schmidt, K.M. and Webb, R.H., 2001, Researchers consider U.S. southwest's response to warmer, drier, conditions: Eos Transactions, American Geophysical Union, 82(41): Oct. 9, p. 475, 478.

Seaber, P.R., Kapinos, F.P., and Knapp, G.L., 1987, Hydrologic Unit Maps: U.S. Geological Survey Water-Supply Paper 2294, 63 p.

Shuttleworth, W.J., 1993, Evaporation: Ch. 4 *in* Handbook of Hydrology, D.R. Maidment (ed.), McGraw-Hill, Inc., p. 4.24.

Stephens, D.B., 1995, Vadose Zone Hydrology: CRC Press, Inc., Boca Raton, Fla., 347 p.

UNESCO, 1979, Map of the world distribution of arid regions: MAB Tech. Notes, no. 7, Paris, 54 p.

U.S. Department of Agriculture – Natural Resource Conservation Service, 1994, State Soil Geographic (STATSGO) Data Base- Data use information: Misc. Pub. no. 1492.

Figure 1. Map showing the aridity classification of groundwater basins in the southwestern United States. Classification based on arid land classification index of the United Nations Educational, Scientific, and Cultural Organization (UNESCO).

Figure 2. Hydrographic areas and subareas within the Great Basin and identifiers.

Figure 3. Schematic of mechanisms controlling net infiltration.

Figure 4. Total mean annual potential recharge, calculated from potential recharge plus potential runoff on a grid cell basis, for basins in the Great Basin.

Figure 5. Total mean annual potential recharge, calculated from potential recharge plus potential runoff as the mean of all grid cells for each basin in the Great Basin.

Figure 6. The ratio of potential in-place recharge to potential runoff, calculated on a grid-cell basis, for basins in the Great Basin, indicating locations where either in-place recharge or runoff are the dominant mechanisms.

Figure 7. The ratio of potential in-place recharge to potential runoff, calculated as the mean of all grid cells for each basin in the Great Basin indicating basins where either in-place recharge or runoff are the dominant mechanisms.

Figure 8. Annual potential recharge, as percentage deviation from the mean potential recharge for 1956–1999 for Continental Lake Valley in the northern part of the Great Basin and the Valjean Valley in the southern part of the Great Basin, indicating differences in recharge for El Niño years owing to negative and positive Pacific Decadal Oscillation (PDO).

Figure 9. Comparison of annual potential recharge, as percentage deviation from the mean potential recharge for 1956-1999, and annual precipitation, as percentage deviation from the mean for 1956-1999 for the Valjean Valley in the southern part of the Great Basin and the Continental Lake Valley in the northern part of the Great Basin.

Figure 10. Total potential recharge, calculated as potential in-place recharge plus 10 percent of potential runoff for 258 basins in the Great Basin determined using several methods of estimating recharge and the basin characterization model (BCM). Range bars indicate inclusion or exclusion of all runoff with in-place recharge.

TABLES

Table 1. Total mean potential recharge (acre-feet/year) calculated for 258 basins in the Great Basin calculated using several methods of estimating recharge and potential in-place recharge and potential runoff calculated several ways using the basin characterization model.

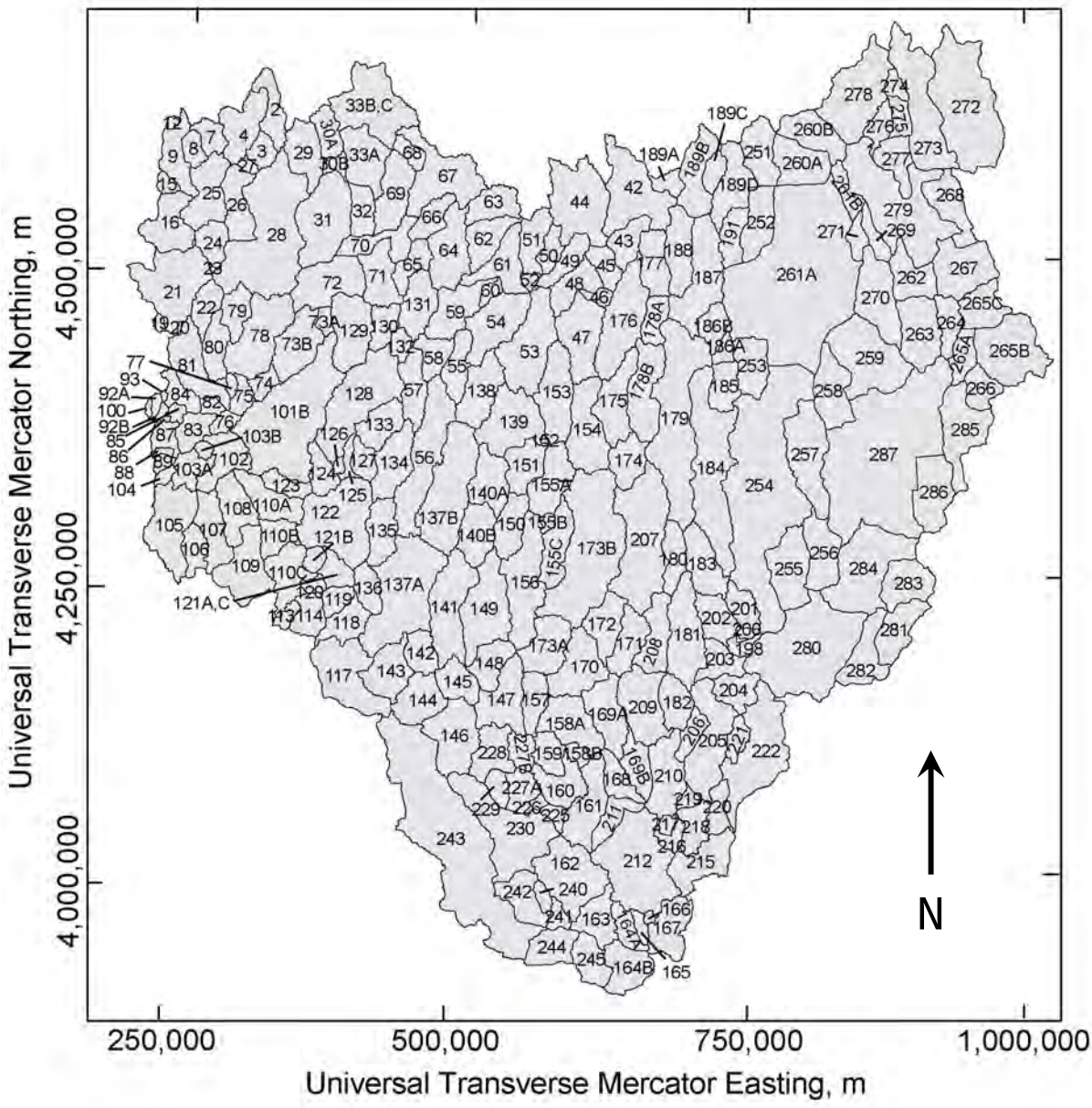

Figure 1. Hydrographic areas and subareas within the Great Basin and identifiers. (From *Harrill and Prudic* [1998])

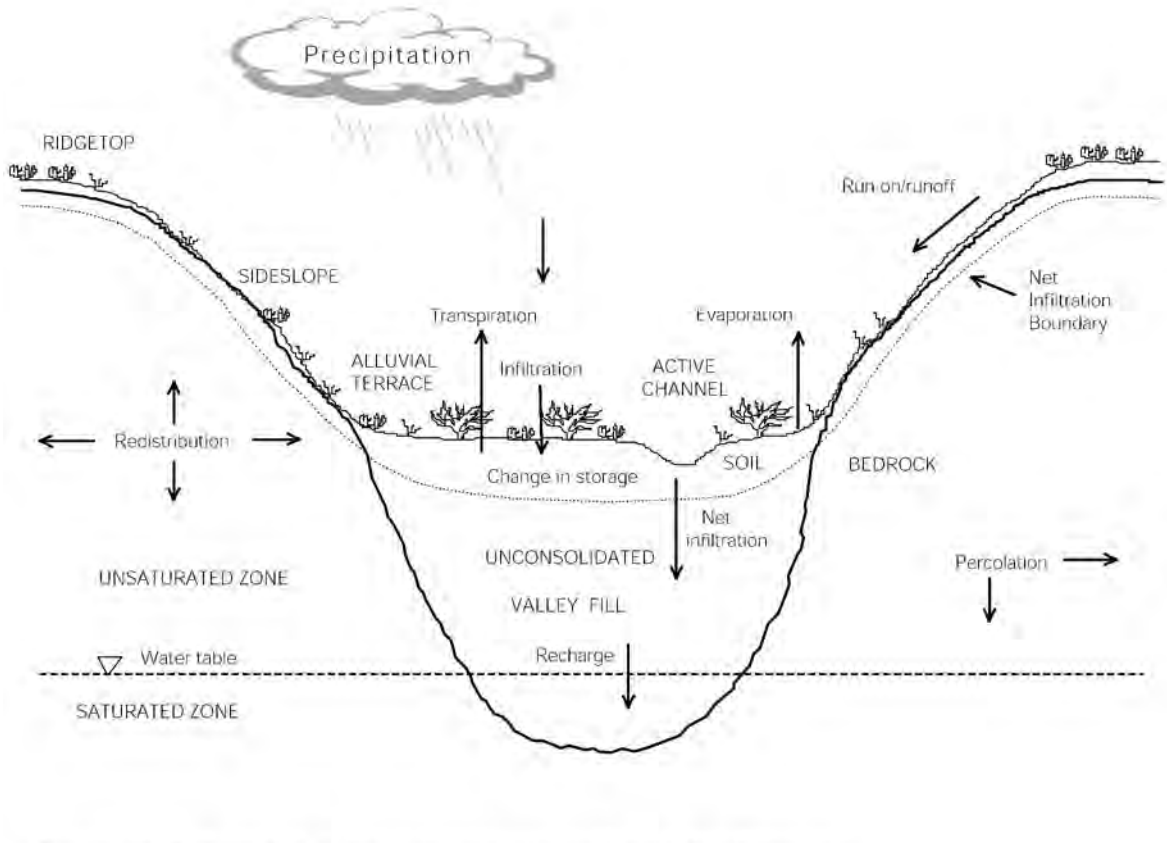

Figure 2. Schematic of mechanisms controlling net infiltration. (From *Hevesi et al.* [2003])

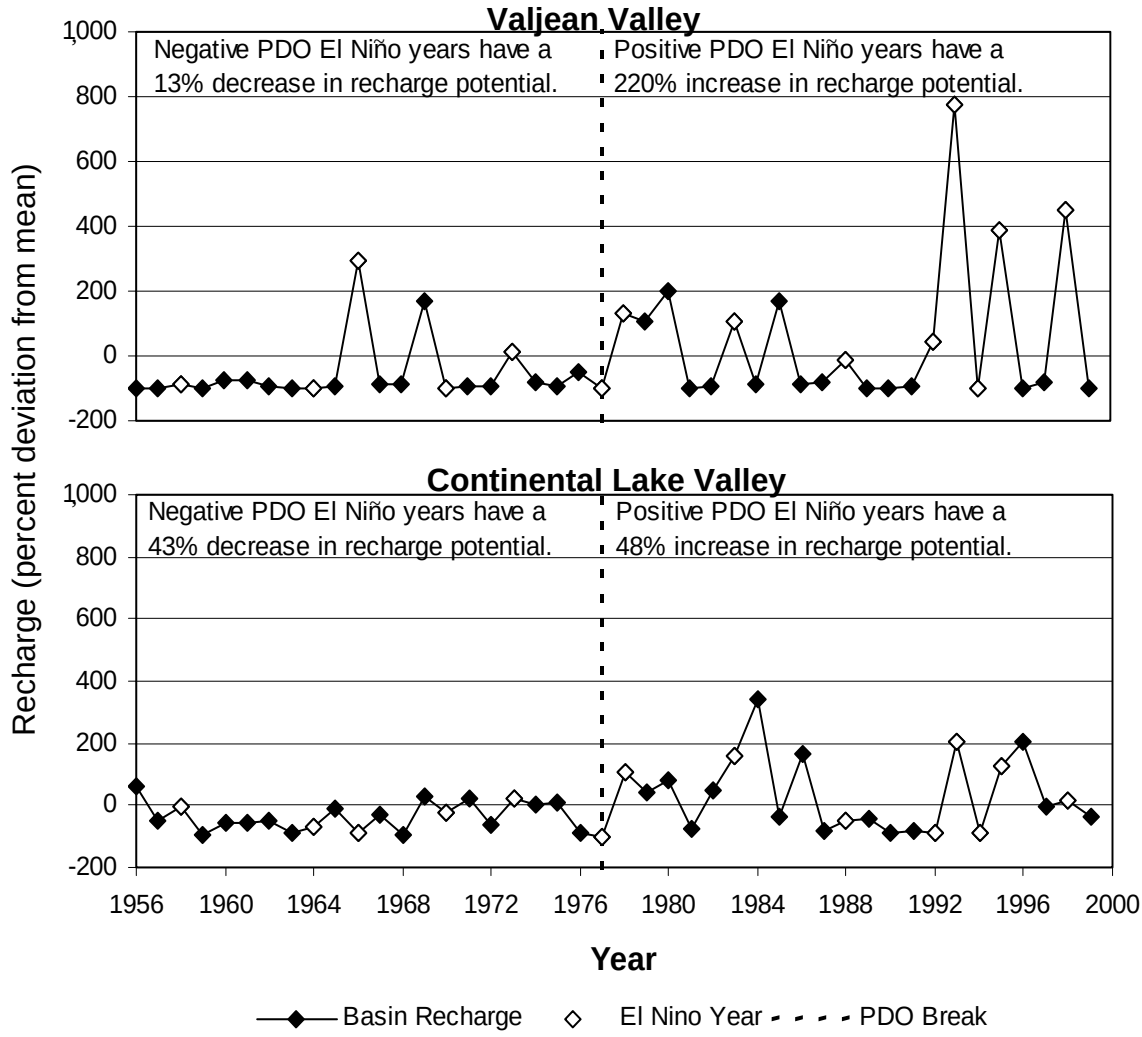

Figure 3. Annual potential recharge, as percentage deviation from the mean potential recharge for 1956–1999 for Continental Lake Valley in the northern part of the Great Basin and the Valjean Valley in the southern part of the Great Basin, indicating differences in recharge for El Niño years owing to negative and positive Pacific Decadal Oscillation (PDO).

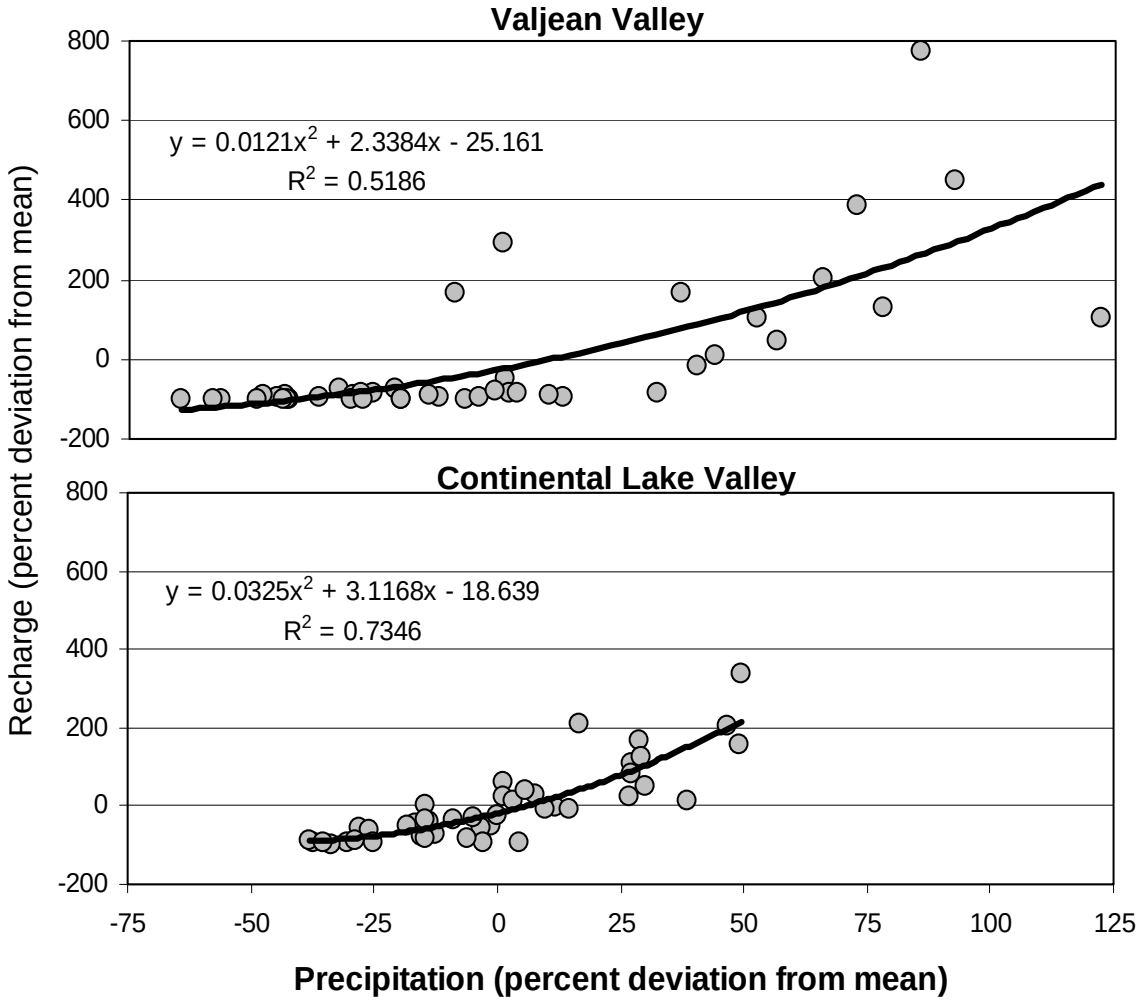

Figure 4. Comparison of annual potential recharge, as percentage deviation from the mean potential recharge for 1956-1999, and annual precipitation, as percentage deviation from the mean for 1956-1999 for the Valjean Valley in the southern part of the Great Basin and the Continental Lake Valley in the northern part of the Great Basin.

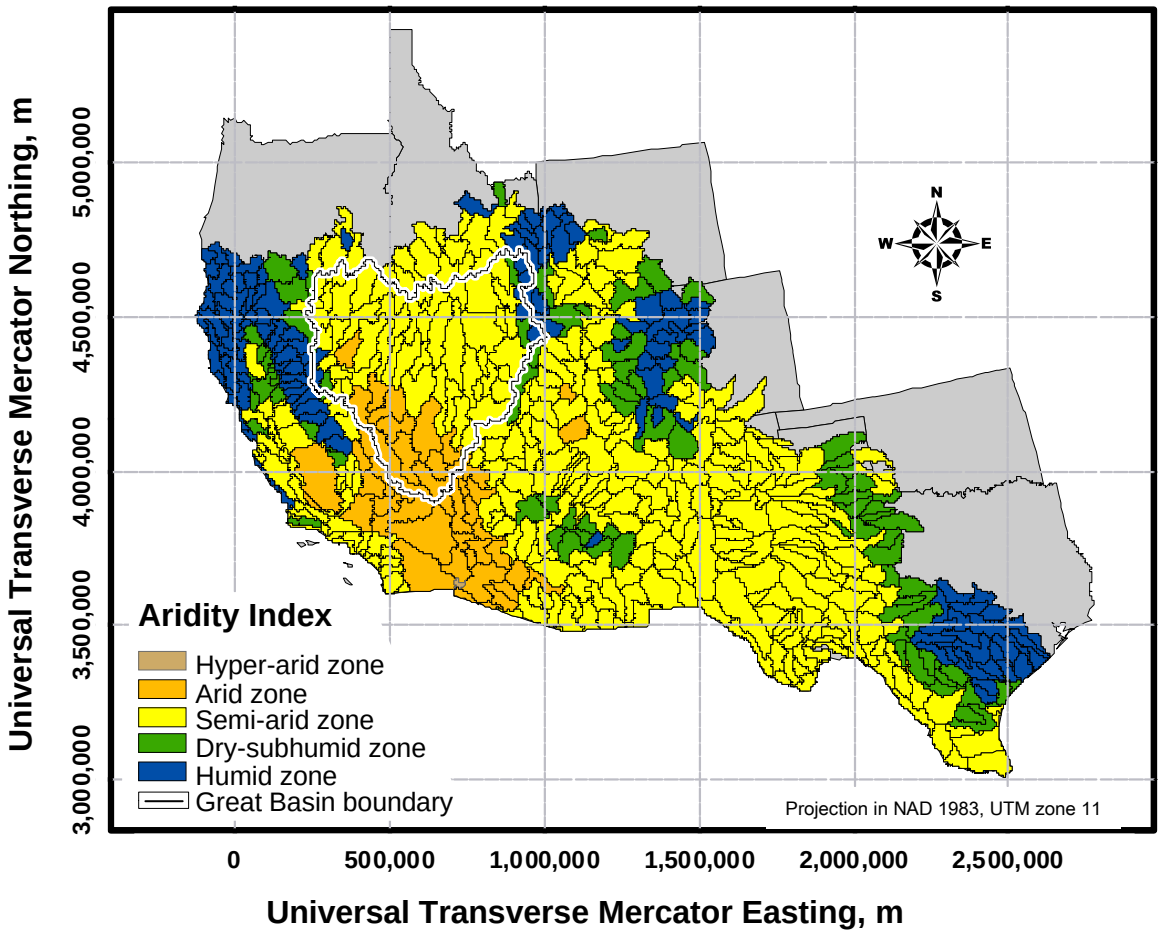

Plate 1. Map showing the aridity classification of ground-water basins in the southwestern United States. Classification based on arid land classification index of the United Nations Educational, Scientific, and Cultural Organization (UNESCO).

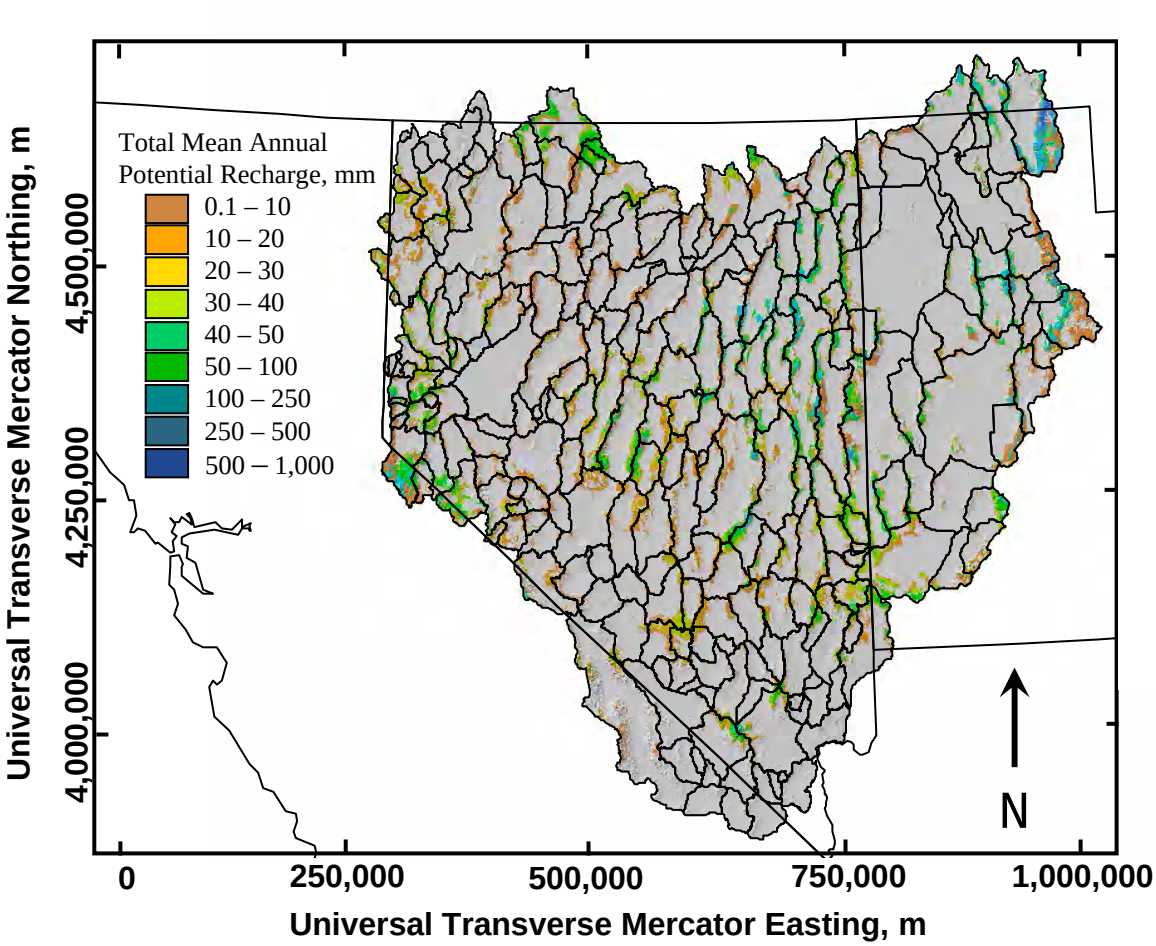

Plate 2. Total mean annual potential recharge, calculated from potential recharge plus potential runoff on a grid cell basis, for basins in the Great Basin.

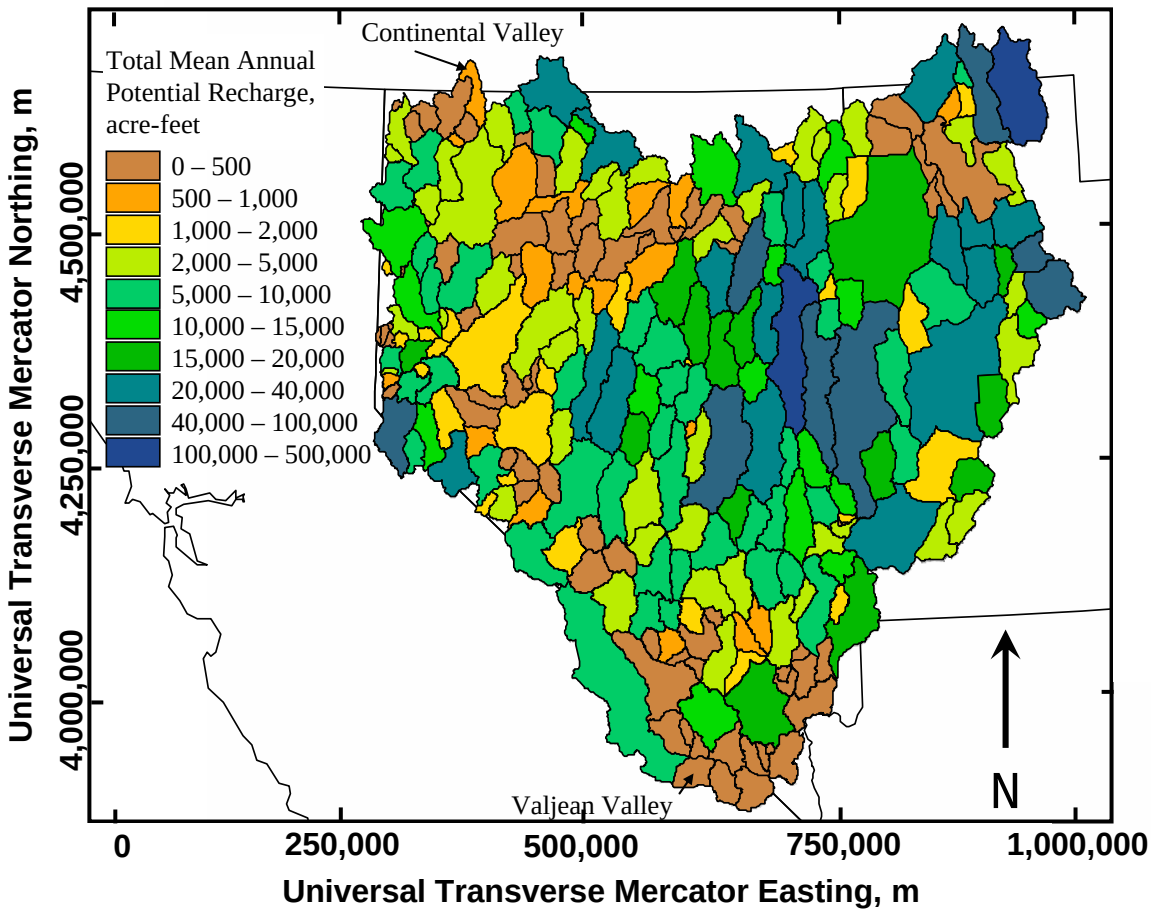

Plate 3. Total mean annual potential recharge, calculated from potential recharge plus potential runoff as the mean of all grid cells for each basin in the Great Basin.

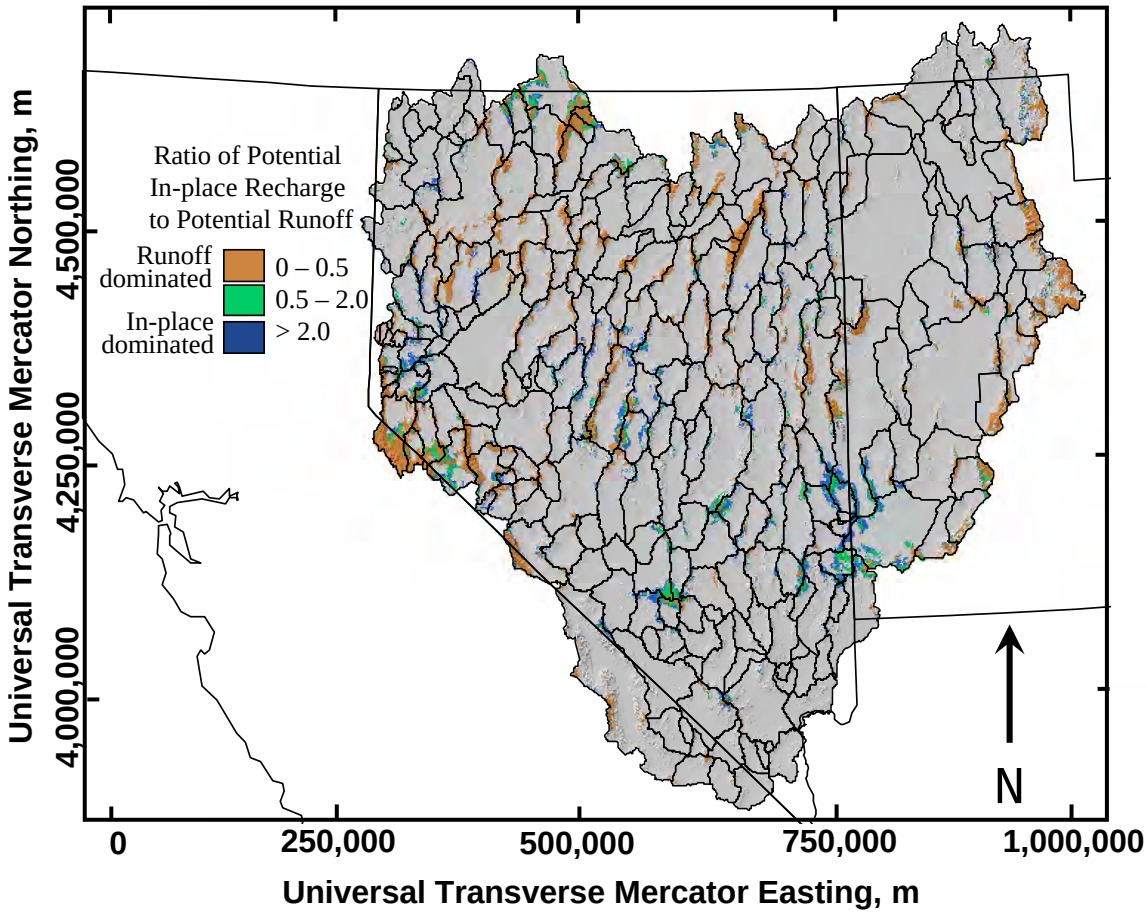

Plate 4. The ratio of potential in-place recharge to potential runoff, calculated on a grid-cell basis, for basins in the Great Basin, indicating locations where either in-place recharge or runoff are the dominant mechanisms.

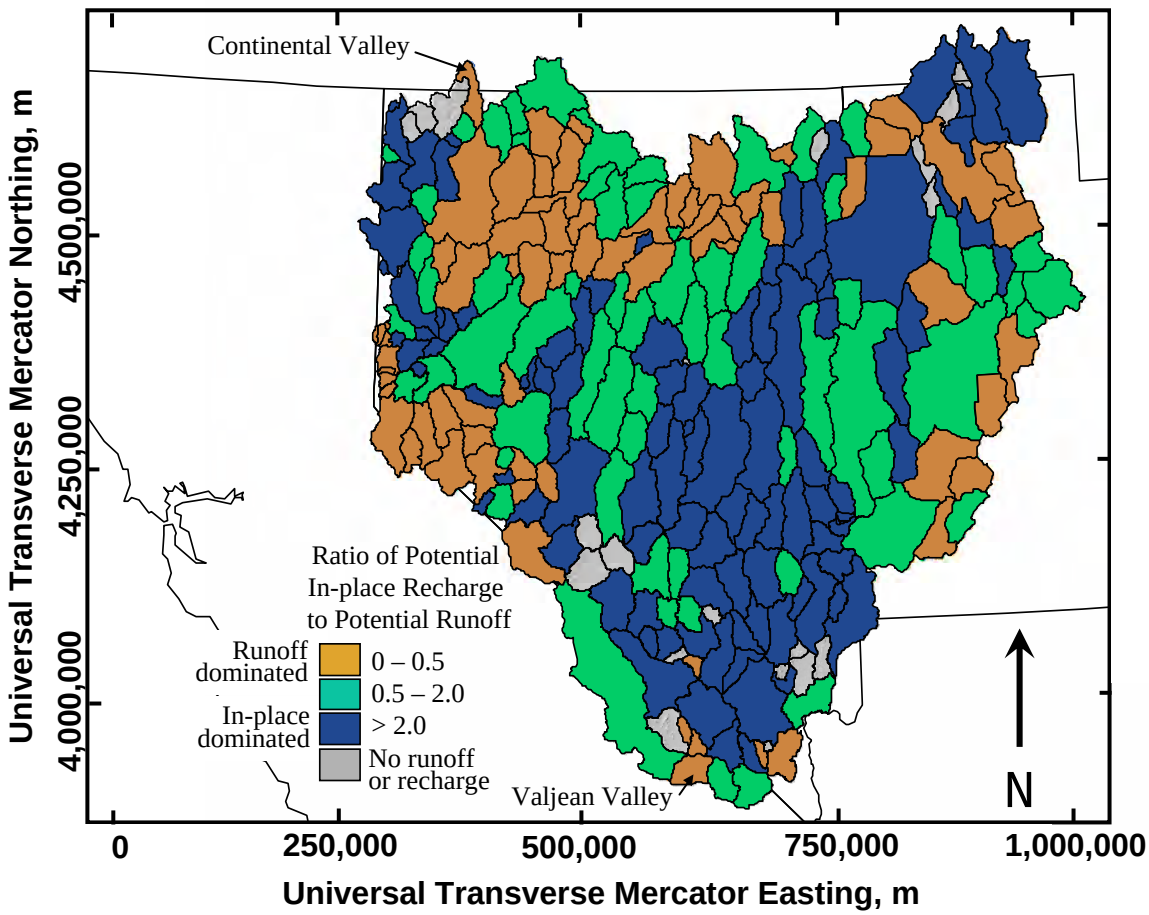

Plate 5. The ratio of potential in-place recharge to potential runoff, calculated as the mean for each basin, for the Great Basin, indicating locations where either runoff of in-place recharge are the dominant mechanisms.

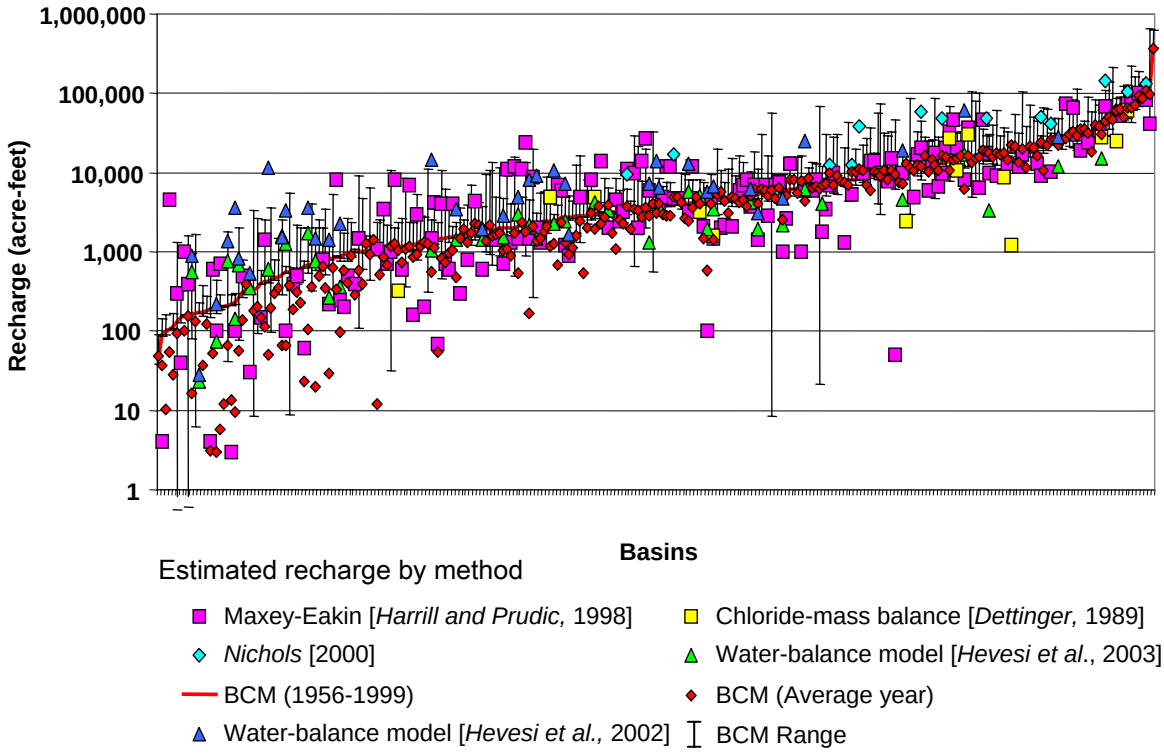

Plate 6. Total potential recharge, calculated as potential in-place recharge plus 10 percent of potential runoff for 258 basins in the Great Basin determined using several methods of estimating recharge and the basin characterization model (BCM). Range bars indicate inclusion or exclusion of all runoff with in-place recharge.

Table 1. Potential recharge (acre-feet/year) calculated for 258 basins in the Great Basin using the basin characterization model (BCM) for in-place recharge and runoff for a mean year and a time series of years, including estimates using the Maxey-Eakin method, chloride-mass balance. Total potential recharge for the Great Basin for BCM estimates shown at the bottom of table.

		Mean potential recharge, in acre-feet per year, by method										
							-------- Basin Characterization Model ---------					
							Mean year			Time series		
Hydro-graphic area or subarea identifier*	Hydrographic area or subarea*	Maxey--Eakin method*	Chloride mass balance method*	Estimates using discharge measure-ments**	Water-balance model (Hevesi et al., 2003)	Water-balance model (Hevesi et al., 2002)	Potential in-place recharge	Potential runoff	Total potential recharge for mean year	Potential in-place recharge	Potential runoff	Total potential recharge for time series
142	Alkali Spring Valley	100			141	3,544	9	0	9	221	82	229
230	Amargosa Desert	1,500			2,139	8,129	146	236	169	1,938	2,567	2,195
151	Antelope Valley (Eureka and Nye)						4,880	1,087	4,988	4,060	1,682	4,228
57	Antelope Valley (Humboldt System)	11,000					2,091	2,289	2,320	1,848	2,988	2,147
93	Antelope Valley (Lemmon Valley)	300					1	947	95	1	1,308	131
186A	Antelope Valley (south)						1,193	486	1,242	977	624	1,039
186B	Antelope Valley (north)						3,574	1,202	3,694	2,897	1,341	3,031
186	Antelope Valley (north and south)	4,700		16,824			4,767	1,688	4,936	3,874	1,965	4,071
106	Antelope Valley (Walker System)	18,000					5,045	75,829	12,627	4,678	82,497	12,928
283	Beaver Valley						15,201	64,886	21,689	15,551	55,149	21,066
280	Beryl-Enterprise Area						25,804	44,431	30,247	21,678	52,721	26,950
137A	Big Smoky Valley (north)	12,000					2,544	2,628	2,807	3,686	3,742	4,060
215	Black Mountains Area	70					51	25	54	1,376	939	1,470
28	Black Rock Desert	14,000					3,963	18,836	5,847	6,055	30,586	9,113
275	Blue Creek Valley	14,000					2,279	59	2,285	3,051	138	3,065
61	Boulder Flat						140	907	231	439	1,569	596
15	Boulder Valley	2,000					5,044	6,228	5,667	4,090	6,382	4,729
75	Bradys Hot Springs Area	160					812	542	866	1,088	1,290	1,216
129	Buena Vista Valley						588	9,755	1,563	670	12,681	1,938
131	Buffalo Valley						284	7,885	1,072	361	8,078	1,169
178A	Butte Valley (north)		2,400				12,653	3,923	13,045	10,465	3,570	10,822
178B	Butte Valley (south)		1,200				21,499	7,413	22,240	17,657	6,261	18,284
178	Butte Valley (north and south)	19,000					34,152	11,336	35,285	28,122	9,831	29,105
272	Cache Valley						339,819	226,765	362,495	372,607	245,166	397,124
148	Cactus Flat	600			1,410	1,969	1,818	1,603	1,978	1,612	2,142	1,826
241	California Valley				775	1,361	13	532	66	41	1,744	216
218	California Wash	60					23	1	23	639	130	652
55	Carico Lake Valley	4,300					1,826	4,080	2,234	1,435	3,582	1,793
101A,B	Carson Desert (Packard and Lahontan Valleys)	1,300					752	1,412	893	1,821	2,218	2,043
105	Carson Valley	41,000					39,856	589,167	98,772	41,627	617,008	103,328
180	Cave Valley	14,000					9,350	9,135	10,264	8,479	9,009	9,380
282	Cedar City Valley						3,275	29,899	6,265	2,696	27,149	5,411
264	Cedar Valley						16,024	12,075	17,231	16,370	12,688	17,639
240	Chicago Valley				569	903	11	57	17	80	873	167
102	Churchill Valley	1,300					6,470	10,420	7,512	6,718	14,298	8,148
143	Clayton Valley	1,500			1,051	14,347	524	306	555	1,300	1,190	1,419
204	Clover Valley (Colorado System)						14,512	17,614	16,274	12,367	20,215	14,389
177	Clover Valley (Independence Valley System)	21,000		58,802			8,065	38,353	11,900	8,223	36,675	11,890
64	Clovers Area						2,250	5,458	2,796	2,493	6,088	3,102
171	Coal Valley	2,000			3,325		3,575	2,643	3,839	2,740	3,701	3,110
100	Cold Springs Valley						7	1,764	184	8	3,355	344
118	Columbus Salt Marsh Valley	700					633	420	675	983	1,207	1,104
2	Continental Lake Valley	11,000					643	4,364	1,079	1,233	7,889	2,022
126	Cowkick Valley						290	91	300	442	352	477
210	Coyote Spring Valley	2,600					5,037	1,467	5,184	5,659	2,924	5,951
229	Crater Flat	220			268	1,424	29	9	30	782	382	820
54	Crescent Valley						1,043	10,935	2,136	910	9,933	1,903
278	Curlew Valley	75,600					26,646	2,177	26,863	26,276	2,728	26,548
103A	Dayton Valley (Carson Plains)						5,522	14,372	6,959	7,090	19,847	9,074
103B	Dayton Valley (Stagecoach Valley)		320				932	990	1,031	1,018	1,357	1,154
103	Dayton Valley (Stagecoach Valley and Carson Plains)	7,900					6,454	15,362	7,991	8,108	21,204	10,228
243	Death Valley	8,000			16,891	60,997	4,960	11,712	6,131	11,755	28,056	14,560
253	Deep Creek Valley	17,000					9,743	25,765	12,319	9,004	23,970	11,401
182	Delamar Valley	1,000					6,627	11,366	7,764	5,308	10,958	6,404
31	Desert Valley	5,000					1,218	12,203	2,438	1,292	15,250	2,817

Table 1. (cont.)

		Mean potential recharge, in acre-feet per year, by method										
							-------- Basin Characterization Model ---------					
							Mean year			Time series		
Hydro-graphic area or subarea identifier*	Hydrographic area or subarea*	Maxey--Eakin method*	Chloride mass balance method*	Estimates using discharge measure-ments**	Water-balance model (Hevesi et al., 2003)	Water-balance model (Hevesi et al., 2002)	Potential in-place recharge	Potential runoff	Total potential recharge for mean year	Potential in-place recharge	Potential runoff	Total potential recharge for time series

Hydrographic area or subarea identifier*	Hydrographic area or subarea*	Maxey--Eakin method*	Chloride mass balance method*	Estimates using discharge measure-ments**	Water-balance model (Hevesi et al., 2003)	Water-balance model (Hevesi et al., 2002)	Potential in-place recharge	Potential runoff	Total potential recharge for mean year	Potential in-place recharge	Potential runoff	Total potential recharge for time series
153	Diamond Valley	21,000	10,500				13,081	20,431	15,124	12,199	19,417	14,141
128	Dixie Valley	6,000					1,909	4,347	2,343	2,199	5,154	2,714
82	Dodge Flat	1,400					1,527	1,460	1,673	1,627	3,337	1,961
181	Dry Lake Valley	5,000					10,307	3,207	10,627	10,666	6,316	11,298
19	Dry Valley (Black Rock Desert System)	200					552	314	584	839	857	925
198	Dry Valley (Colorado System)						2,065	1,278	2,192	1,555	2,603	1,815
16	Duck Lake Valley	9,000	8,900				16,185	11,988	17,384	16,060	20,458	18,106
259	Dugway-Government Creek Valley	7,000					4,489	17,112	6,200	3,714	14,735	5,187
104	Eagle Valley (Carson System)	8,700					219	18,933	2,112	266	19,625	2,228
200	Eagle Valley (Colorado System)						810	796	890	848	1,508	999
268	East Shore Area						3,530	98,590	13,389	4,993	101,225	15,116
109	East Walker Area	31,000					21,032	84,308	29,463	19,215	92,571	28,472
127	Eastgate Valley Area						1,032	1,319	1,164	1,194	1,707	1,364
133	Edwards Creek Valley	8,000					2,722	3,453	3,067	2,503	4,239	2,927
167	Eldorado Valley	1,100					1	112	12	933	1,384	1,072
49	Elko Segment						244	3,823	626	340	4,909	831
158A	Emigrant Valley (Groom Lake Valley)	3,200			5,739	12,910	2,279	1,409	2,420	3,655	4,574	4,112
158B	Emigrant Valley (Papoose Lake Valley)	4					2	7	3	151	359	187
124	Fairview Valley	500					124	163	140	265	521	317
76	Fernley Area	600					888	647	953	1,307	2,001	1,507
77	Fireball Valley	200					1,239	968	1,336	1,213	1,563	1,369
117	Fish Lake Valley	33,000	26,800				5,855	48,812	10,737	7,743	60,393	13,783
258	Fish Springs Flat	4,000					1,016	384	1,054	1,460	664	1,526
227A	Fortymile Canyon (Jackass Flat)	900			1,583	1,665	857	535	910	2,524	2,535	2,778
227B	Fortymile Canyon (Buckboard Mesa)	1,400			1,959	3,113	3,727	3,287	4,056	4,684	6,436	5,327
160	Frenchman Flat	100			1,903	5,683	537	396	576	4,299	2,207	4,520
122	Gabbs Valley	5,000	4,900				1,023	1,238	1,147	2,195	2,367	2,431
172	Garden Valley	10,000			3,323		16,542	14,325	17,974	13,866	16,939	15,559
120	Garfield Flat	300					1,371	1,257	1,497	1,382	2,265	1,609
216	Garnet Valley	400					288	60	294	989	109	1,000
147	Gold Flat	3,800			4,205	6,287	4,637	3,701	5,007	4,595	5,847	5,180
187	Goshute Valley	10,400		40,911			25,210	9,048	26,115	22,410	9,498	23,360
23	Granite Basin	400					1	1,535	154	1	1,599	160
78	Granite Springs Valley	3,500					5,044	22,631	7,307	5,046	25,213	7,567
138	Grass Valley	13,000					6,891	11,266	8,018	5,030	10,926	6,123
71	Grass Valley (Humboldt System)	12,000					410	13,387	1,749	502	15,453	2,048
279	Great Salt Lake						3	1,320	135	6	1,647	171
261B	Great Salt Lake Desert (east)	4,500					54	0	54	106	0	106
261A	Great Salt Lake Desert (west)	47,000					14,026	4,685	14,494	13,365	5,116	13,876
3	Gridley Lake Valley	4,500					933	1,666	1,099	2,588	5,981	3,186
251	Grouse Creek Valley	14,000					2,369	3,490	2,718	3,265	4,606	3,726
276	Hansel and North Rozel Flat	8,000					331	4	332	864	28	867
68	Hardscrabble Area	9,000					12,833	46,734	17,506	12,248	48,868	17,134
217	Hidden Valley (north)	400					188	6	188	566	57	571
166	Hidden Valley (south)				23	28	0	0	-	169	63	175
25	High Rock Lake Valley	13,000					13,762	8,367	14,599	16,559	16,145	18,173
156	Hot Creek Valley	7,000		5,756			4,512	1,805	4,692	5,380	4,034	5,783
24	Hualapai Flat	7,000					3,700	7,727	4,473	4,088	9,248	5,013
47	Huntington Valley						34,668	59,713	40,639	29,248	52,667	34,514
113	Huntoon Valley	800					1,226	1,012	1,327	1,440	2,439	1,683
72	Imlay Area	4,000					226	6,056	831	462	10,260	1,488
188	Independence Valley	9,300		50,065			22,907	8,347	23,742	20,525	8,863	21,411
161	Indian Springs Valley	10,000			4,591	18,978	6,912	3,904	7,302	9,966	7,901	10,756
135	Ione Valley	8,000					1,176	689	1,245	1,026	984	1,125
164A	Ivanpah Valley (north)				1,399	3,482	438	418	480	1,487	896	1,576
164B	Ivanpah Valley (south)				1,569	1,519	53	126	66	293	2,261	519
164	Ivanpah Valley (North and South)	1,500			2,968	5,001	491	545	546	1,779	3,158	2,095
174	Jakes Valley			38,203			10,761	2,131	10,974	8,082	2,280	8,310
165	Jean Lake Valley	100			73	217	0	28	3	167	276	195

Table 1. (cont.)

	Mean potential recharge, in acre-feet per year, by method					
				-------- Basin Characterization Model ---------		
				Mean year		Time series

Hydrographic area or subarea identifier*	Hydrographic area or subarea*	Mean potential recharge, in acre-feet per year, by method										
		Maxey--Eakin method*	Chloride mass balance method*	Estimates using discharge measure-ments**	Water-balance model (Hevesi et al., 2003)	Water-balance model (Hevesi et al., 2002)	Potential in-place recharge	Potential runoff	Total potential recharge for mean year	Potential in-place recharge	Potential runoff	Total potential recharge for time series
132	Jersey Valley	800					557	955	652	677	1,366	813
206	Kane Springs Valley						4,579	8,416	5,421	5,262	10,659	6,328
157	Kawich Valley	3,500			3,688	6,563	3,788	3,008	4,089	3,454	5,143	3,968
66	Kelly Creek Area						3,730	5,497	4,279	3,408	6,654	4,073
30A	Kings River Valley (Rio King Subarea)						8,386	21,333	10,520	7,698	24,428	10,141
30B	Kings River Valley (Sodhouse Subarea)						26	23	28	109	62	116
30	Kings River Valley (Rio King and Sodhouse subareas)	15,000					8,412	21,357	10,547	7,808	24,490	10,257
139	Kobeh Valley						7,793	5,852	8,378	5,942	5,413	6,483
79	Kumiva Valley	1,000					36	11,208	1,157	31	10,742	1,105
183	Lake Valley	13,000					13,213	15,049	14,718	10,858	14,946	12,353
45	Lamoille Valley						20	62,875	6,308	21	69,928	7,014
212	Las Vegas Valley		28,000		15,147		28,072	21,349	30,207	33,697	28,483	36,545
285	Leamington Canyon						3,786	31,981	6,984	4,388	38,152	8,203
92A	Lemmon Valley (west						8	3,787	386	9	5,521	561
92B	Lemmon Valley (east						7	1,906	197	99	3,519	451
92	Lemmon Valley (east and west	1,500					14	5,693	584	108	9,040	1,012
144	Lida Valley				610	11,335	50	6	50	406	118	418
150	Little Fish Lake Valley	11,000		9,628			3,501	2,996	3,801	3,010	3,131	3,324
67	Little Humboldt Valley	24,000					26,022	58,057	31,828	25,338	64,651	31,803
155A	Little Smoky Valley (north)						7,881	1,466	8,028	6,122	1,561	6,278
155B	Little Smoky Valley (central)						391	93	400	317	167	334
155C	Little Smoky Valley (south)						1,889	567	1,946	1,542	963	1,638
155	Little Smoky Valley (north, central and south)	5,400		12,681			10,161	2,126	10,374	7,981	2,692	8,250
9	Long Valley	6,000					5,908	5,164	6,424	5,913	7,486	6,662
175	Long Valley (Colorado System)	10,000		47,740			15,875	4,139	16,289	13,186	3,495	13,536
73A	Lovelock Valley (Oreana Subarea)						39	1,672	206	95	2,542	349
73B	Lovelock Valley (Upper and Lower Valley subareas)						1,732	2,826	2,015	2,290	5,810	2,871
73	Lovelock Valley (Orena, and Upper and Lower Valley subareas)	3,200					1,771	4,498	2,220	2,385	8,352	3,220
242	Lower Amargosa Valley				767	1,475	17	26	20	590	1,420	732
205	Lower Meadow Valley Wash						10,883	8,004	11,683	18,126	19,659	20,092
220	Lower Moapa Valley	40					0	0	-	128	193	147
59	Lower Reese River Valley						354	5,804	935	445	5,995	1,044
51	Maggie Creek Area						695	8,759	1,571	1,748	10,529	2,801
273	Malad-Lower Bear River Area						81,639	43,703	86,010	84,159	44,066	88,566
52	Marys Creek Area						35	17	37	154	228	176
42	Marys River Area						19,014	36,806	22,694	18,977	43,651	23,342
108	Mason Valley	2,000					1,438	19,162	3,354	1,635	19,694	3,604
8	Massacre Lake Valley						1,086	247	1,110	2,613	1,829	2,796
225	Mercury Valley	250			359	2,256	75	243	99	751	1,165	867
163	Mesquite Valley	1,500	1,600		3,470	6,696	1,370	582	1,428	4,328	2,492	4,577
58	Middle Reese River Valley	7,000					1,065	1,119	1,177	1,045	1,274	1,173
284	Milford Area						1,509	6,091	2,118	1,734	6,919	2,426
140A	Monitor Valley (north)						8,536	15,375	10,074	6,981	12,882	8,269
140B	Monitor Valley (south)						13,827	22,150	16,042	10,260	17,665	12,026
136	Monte Cristo Valley	500					190	1,179	308	399	1,756	575
12	Mosquito Valley	700					6	1	6	185	106	196
26	Mud Meadows	8,000					3,439	3,346	3,774	4,590	4,711	5,061
219	Muddy River Springs Area						12	0	12	207	1	207
154	Newark Valley	17,500		49,092			16,721	17,077	18,428	13,852	15,380	15,390
44	North Fork Area						7,189	34,246	10,614	17,330	49,380	22,268
137B	Northern Big Smoky Valley	65,000					25,680	70,153	32,695	20,720	62,976	27,018
266	Northern Juab Valley						12,996	24,774	15,474	12,878	27,698	15,648
228	Oasis Valley	1,000			2,209	4,698	2,445	744	2,519	5,512	3,919	5,903
209	Pahranagat Valley	1,800			4,046		6,620	4,234	7,043	6,665	5,211	7,186
208	Pahroc Valley	2,200					4,275	1,564	4,432	4,531	3,015	4,832
162	Pahrump Valley				11,759	28,437	20,976	17,319	22,708	23,716	25,591	26,275
203	Panaca Valley						4,535	2,059	4,741	4,506	4,779	4,984
69	Paradise Valley	10,000					2,902	63,905	9,293	2,971	70,503	10,022
260B	Park Valley (east)						256	10,171	1,273	317	10,772	1,394

Table 1. (cont.)

Hydrographic area or subarea identifier*	Hydrographic area or subarea*	Maxey--Eakin method*	Chloride mass balance method*	Estimates using discharge measure-ments**	water-balance model (Hevesi et al., 2003)	water-balance model (Hevesi et al., 2002)	-------- Basin Characterization Model --------- Mean year Potential in-place recharge	Potential runoff	Total potential recharge for mean year	Time series Potential in-place recharge	Potential runoff	Total potential recharge for time series
260A	Park Valley (west)						319	1,736	493	585	1,923	777
260	Park Valley (east and west)	24,000					575	11,907	1,765	902	12,696	2,171
281	Parowan Valley						6,718	24,701	9,188	5,368	24,572	7,825
202	Patterson Valley	8,000					6,201	4,427	6,643	6,046	7,132	6,759
286	Pavant Valley						20,068	56,338	25,701	19,957	64,934	26,450
170	Penoyer Valley	4,300	3,200		5,160		3,797	2,551	4,052	3,828	4,460	4,275
191	Pilot Creek Valley	2,400					2,239	2,778	2,517	2,871	3,187	3,189
252	Pilot Valley	3,400					613	2,543	867	837	2,551	1,092
29	Pine Forest Valley	10,000					5,493	15,310	7,024	5,452	23,193	7,771
255	Pine Valley (Great Salt Lake Desert System)	21,000					14,027	18,308	15,858	11,982	16,365	13,619
53	Pine Valley (Humboldt System)	46,000					16,331	27,297	19,060	13,026	23,031	15,330
130	Pleasant Valley (Dixie Valley System)	3,000					601	3,188	920	801	4,544	1,256
88	Pleasant Valley (Truckee System)	10,000					746	27,585	3,505	663	28,877	3,550
274	Pocatello Valley						7,766	102	7,777	8,008	121	8,020
277	Promontory Mountains Area						1,888	490	1,937	3,373	954	3,468
65	Pumpernickel Valley						101	2,591	360	321	3,754	697
81	Pyramid Lake Valley	6,600					9,830	9,656	10,796	11,443	16,877	13,130
33A	Quinn River Valley (Orovada Subarea)						8,128	68,406	14,969	7,865	73,280	15,193
33B,C	Quinn River Valley (McDermitt and Oregon Canyon)						40,294	103,185	50,612	35,080	103,920	45,472
33	Quinn River Valley (Orovada, McDermitt, and Oregon Canyon subareas)	73,000					48,422	171,590	65,581	42,945	177,200	60,665
173A	Railroad Valley (south)		4,900		4,135		1,853	892	1,942	2,682	2,539	2,936
173B	Railroad Valley (north)		24,800	61,083			57,421	39,280	61,349	46,876	38,659	50,742
173	Railroad Valley (north and south)	52,000					59,274	40,172	63,291	49,558	41,199	53,678
141	Ralston Valley	5,000					3,708	3,683	4,076	4,028	5,410	4,568
123	Rawhide Flats	150					144	42	149	394	179	412
119	Rhodes Salt Marsh Valley	500					318	882	406	756	1,880	944
62	Rock Creek Valley						442	849	527	921	1,581	1,079
226	Rock Valley	30			352	532	0	0	-	324	110	335
199	Rose Valley						48	4	48	38	52	43
176	Ruby Valley	68,000		145,636			35,382	88,306	44,212	29,133	82,288	37,362
263	Rush Valley	34,000					33,806	42,371	38,043	31,493	40,184	35,511
267	Salt Lake Valley						28,193	182,454	46,439	29,827	184,549	48,282
22	San Emidio Desert	2,100					3,862	9,961	4,858	3,747	11,559	4,903
20	Sano Valley	4					37	2	37	87	54	93
146	Sarcobatus Flat	1,200			2,466	7,315	1,230	707	1,301	2,532	2,398	2,772
287	Sevier Desert						17,238	30,771	20,316	17,924	33,064	21,230
245	Shadow Valley				1,731	3,634	89	145	104	528	1,506	679
32	Silver State Valley	1,400					52	634	115	183	2,344	418
271	Sink Valley	1,000					99	0	99	154	5	154
270	Skull Valley						16,969	44,502	21,419	14,624	39,740	18,598
134	Smith Creek Valley	12,000					3,279	2,935	3,572	3,738	4,550	4,193
107	Smith Valley	17,000					11,313	87,974	20,111	10,359	94,692	19,828
21	Smoke Creek Desert	13,000					14,993	14,351	16,428	18,729	25,829	21,311
254	Snake Valley	100,000					80,079	126,490	92,728	69,738	122,176	81,955
121A,C	Soda Spring Valley (east and central)						242	1,483	390	598	4,188	1,017
121B	Soda Spring Valley (west)						257	871	344	367	1,108	478
121	Soda Spring Valley (east, central, and west)	700					499	2,354	735	965	5,297	1,494
46	South Fork Area						8	59,056	5,914	8	55,920	5,600
85	Spanish Springs Valley	600					695	474	743	991	1,685	1,159
201	Spring Valley (Colorado System)	10,000					9,549	13,249	10,874	7,486	14,436	8,930
184	Spring Valley (Great Salt Lake Desert System)	75,000	61,600	103,569			57,629	93,577	66,987	48,116	80,635	56,179
43	Starr Valley Area						2,905	84,762	11,381	2,986	82,405	11,226
179	Steptoe Valley	85,000		131,469			104,285	71,344	111,419	88,282	61,094	94,391
152	Stevens Basin						1,390	10	1,391	1,055	113	1,067
125	Stingaree Valley						9	13	10	90	73	97
149	Stone Cabin Valley	5,000					2,843	1,628	3,006	3,673	3,139	3,987
145	Stonewall Flat	100			1,241	3,393	65	6	65	540	110	551
27	Summit Lake Valley	4,200					1,000	1,072	1,107	1,248	2,204	1,469
86	Sun Valley	50					5,657	36,757	9,333	6,260	40,549	10,315
50	Susie Creek Area						178	1,684	346	525	2,907	816

Table 1. (cont.)

Hydrographic area or subarea identifier*	Hydrographic area or subarea*	Mean potential recharge, in acre-feet per year, by method										
							-------- Basin Characterization Model ---------					
							Mean year			Time series		
		Maxey--Eakin method*	Chloride mass balance method*	Estimates using discharge measure-ments**	Water-balance model (Hevesi et al., 2003)	Water-balance model (Hevesi et al., 2002)	Potential in-place recharge	Potential runoff	Total potential recharge for mean year	Potential in-place recharge	Potential runoff	Total potential recharge for time series
7	Swan Lake Valley						514	248	539	2,697	1,688	2,866
114	Teels Marsh Valley	1,300					1,284	1,887	1,473	2,035	3,527	2,387
48	Tenmile Creek Area						3,608	17,122	5,320	2,954	16,702	4,624
189A	Thousand Springs Valley (Herrell Siding-Brush Creek subarea)						1,192	5,092	1,701	1,197	5,707	1,768
189B	Thousand Springs Valley (Toano-Rock Spring subarea)						2,206	4,322	2,638	3,505	5,960	4,101
189C	Thousand Springs Valley (Rocky Butte subarea)						1,728	0	1,728	3,160	74	3,167
189D	Thousand Springs Valley (Montello-Crittenden Creek subarea)						7,573	358	7,609	10,436	1,462	10,582
189	Thousand Springs Valley (Herrell Siding-Brush Creeak, Toano-Rock Spring, Rocky Butte and Montello-Crittenden Creek subareas)	12,000					12,699	9,772	13,676	18,299	13,202	19,619
168	Three Lakes Valley (north)	2,000			1,490	9,031	1,317	472	1,364	2,182	903	2,272
211	Three Lakes Valley (south)	6,000			1,298	7,335	2,725	1,773	2,903	3,631	1,981	3,830
169A	Tikapoo Valley (north)				3,971	13,767	3,028	947	3,123	3,756	2,050	3,961
169B	Tikapoo Valley (south)				2,295	10,819	1,230	263	1,256	2,419	581	2,477
169	Tikapoo Valley (north and south)	6,000			6,266	24,586			-			-
185	Tippett Valley	6,900		12,389			9,364	3,534	9,717	7,367	2,918	7,659
137A	Tonopah Flat	12,000					2,544	2,628	2,807	3,686	3,742	4,060
262	Tooele Valley						23,941	24,445	26,386	23,885	23,766	26,262
83	Tracy Segment	6,000					9,768	6,750	10,443	10,613	14,424	12,056
87	Truckee Meadows	27,000					1,983	15,837	3,566	2,013	17,699	3,783
221	Tule Desert	2,100					1,319	1,512	1,470	4,126	3,456	4,472
257	Tule Valley	7,600					6,206	2,992	6,505	5,559	2,736	5,833
56	Upper Reese River Valley	37,000	30,000				13,529	30,683	16,598	12,137	29,699	15,107
265A	Utah Valley Area (Goshen Valley						1,561	2,526	1,814	2,056	3,630	2,419
265C	Utah Valley Area (north)						42,897	76,850	50,582	45,816	78,973	53,714
265B	Utah Valley Area (south)						62,634	85,648	71,199	63,401	94,892	72,890
244	Valjean Valley				671	820	2	533	56	77	1,921	269
222	Virgin River Valley						16,014	23,837	18,398	29,392	30,078	32,400
4	Virgin Valley	7,000					615	615	676	2,377	1,561	2,533
256	Wah Wah Valley	7,000					5,869	1,886	6,057	5,186	2,319	5,418
110A	Walker Lake Valley (Schurz Subarea)						351	13,684	1,720	897	10,780	1,975
110B	Walker Lake Valley (Lake Subarea)						487	35,034	3,991	560	32,806	3,841
110C	Walker Lake Valley (Whiskey Flat·						4,599	54,355	10,035	4,096	53,332	9,429
110	Walker Lake Valley	6,500					5,438	103,074	15,745	5,553	96,918	15,245
84	Warm Springs Area	6,000					3,446	7,044	4,150	3,738	12,722	5,010
269	West Shore Area	600					53	1	53	188	6	189
60	Whirlwind Valley						119	55	125	169	104	179
74	White Plains	3					13	0	13	212	80	220
207	White River Valley						33,443	14,818	34,925	29,192	15,673	30,759
63	Willow Creek Valley						2,629	5,052	3,134	4,189	6,954	4,885
80	Winnemucca Lake Valley	2,900					4,099	9,894	5,088	4,292	11,791	5,471
70	Winnemucca Segment						622	7,321	1,354	990	8,478	1,838
159	Yucca Flat	700			1,557	2,815	874	1,732	1,047	1,677	3,002	1,977
	Total potential Great Basin recharge						2,406,022	4,828,227	2,888,844	2,428,874	5,239,825	2,952,856

* Harrill and Prudic (1998)

** Nichols (2000)